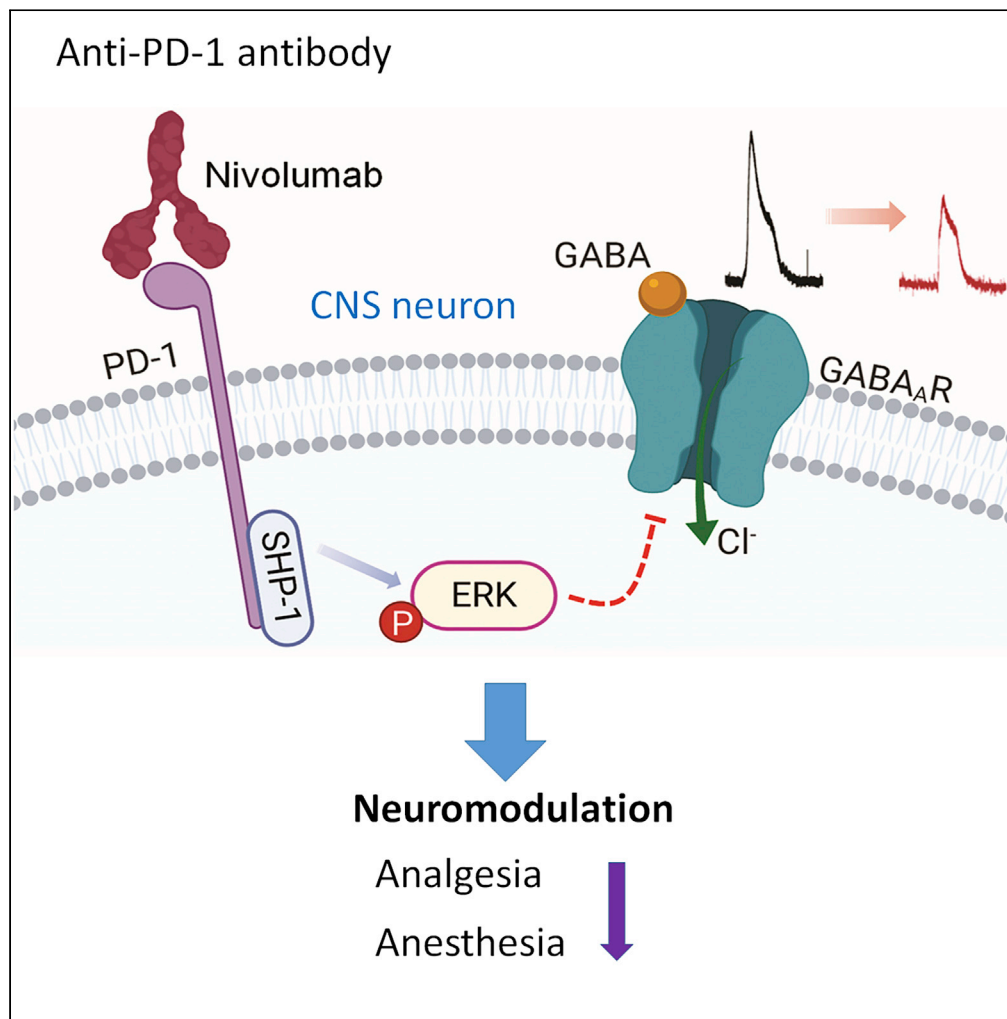


Article

PD-1 Regulates GABAergic Neurotransmission and GABA-Mediated Analgesia and Anesthesia



Changyu Jiang,
Zilong Wang,
Christopher R.
Donnelly, ...,
Megumi Matsuda,
Junli Zhao, Ru-
Rong Ji

ru-rong.ji@duke.edu

HIGHLIGHTS

Pd1 mRNA and PD-1 protein are widely expressed in spinal cord and brain neurons

GABA-induced currents in CNS neurons are suppressed by PD-1 blockade with Nivolumab

Nivolumab binds neuronal PD-1 to induce ERK activation and GABAergic inhibition

GABA-mediated pain inhibition and anesthesia is impaired after *Pd1* deficiency

Jiang et al., iScience 23,
101570
October 23, 2020 © 2020 The
Author(s).
[https://doi.org/10.1016/
j.isci.2020.101570](https://doi.org/10.1016/j.isci.2020.101570)

Article

PD-1 Regulates GABAergic Neurotransmission and GABA-Mediated Analgesia and Anesthesia

Changyu Jiang,¹ Zilong Wang,¹ Christopher R. Donnelly,¹ Kaiyuan Wang,¹ Amanda S. Andriessen,¹ Xueshu Tao,¹ Megumi Matsuda,¹ Junli Zhao,¹ and Ru-Rong Ji^{1,2,3,4,*}

SUMMARY

The immune checkpoint inhibitor programmed cell death protein 1 (PD-1) plays a critical role in immune regulation. Recent studies have demonstrated functional PD-1 expression in peripheral sensory neurons, which contributes to neuronal excitability, pain, and opioid analgesia. Here we report neuronal expression and function of PD-1 in the central nervous system (CNS), including the spinal cord, thalamus, and cerebral cortex. Notably, GABA-induced currents in spinal dorsal horn neurons, thalamic neurons, and cortical neurons are suppressed by the PD-1-neutralizing immunotherapeutic Nivolumab in spinal cord slices, brain slices, and dissociated cortical neurons. Reductions in GABA-mediated currents in CNS neurons were also observed in *Pd1*^{-/-} mice without changes in GABA receptor expression. Mechanistically, Nivolumab binds spinal cord neurons and elicits ERK phosphorylation to suppress GABA currents. Finally, both GABA-mediated analgesia and anesthesia are impaired by *Pd1* deficiency. Our findings reveal PD-1 as a CNS-neuronal inhibitor that regulates GABAergic signaling and GABA-mediated behaviors.

INTRODUCTION

Programmed cell death protein-1 (PD-1), also known as cluster of differentiation 279 (CD279), is a member of the immunoglobulin gene superfamily. PD-1 was discovered during a screening for genes involved in apoptosis (Ishida et al., 1992). The PD-1 protein in humans is encoded by the *PDCD1* gene (Shinohara et al., 1994). As PD-1 is expressed by T cells, B cells, and myeloid cells, mice lacking PD-1 (encoded by *Pdcd1/Pd1*) exhibit impaired immune tolerance and autoimmune features (Nishimura et al., 1999). Engagement of the PD-1 receptor with its ligand PD-L1, a T cell co-stimulatory molecule (Dong et al., 1999), leads to negative regulation of lymphocyte activation (Freeman et al., 2000). Immunotherapies using anti-PD-1 monoclonal antibodies have become the gold standard in treating various cancers (Brahmer et al., 2012; Herbst et al., 2014). Immunotherapy was also shown to improve Alzheimer disease, through activation of macrophages and clearance of cerebral amyloid- β plaques (Baruch et al., 2016), although this has been disputed (Latta-Mahieu et al., 2018).

Although neurons and immune cells are each unique cell types with regard to their morphology, gene expression, and function, primary sensory neurons in the dorsal root ganglion (DRG) express various immune regulatory proteins such as cytokines, cytokine receptors, and Toll-like receptors classically associated with host defense (Chiu et al., 2012; Donnelly et al., 2020; Liu et al., 2010; Talbot et al., 2016). We recently demonstrated that DRG nociceptive neurons of the peripheral nervous system (PNS) express functional PD-1 (Chen et al., 2017; Wang et al., 2020b). *Pd1*-deficient mice show hyperexcitability in sensory neurons and hypersensitivity to pain (Chen et al., 2017). PD-1 co-expression with mu opioid receptors in DRG neurons also regulates morphine analgesia (Wang et al., 2020b). It remains unknown whether neuronal PD-1 also plays an active role in the central nervous system (CNS). In this study we found that *Pd1* mRNA and PD-1 protein are widely expressed by neurons in the spinal cord and different brain regions. GABAergic neurons are a major type of inhibitory neurons in the spinal cord and act as a gate control of pain (Braz et al., 2014; Melzack and Wall, 1965). GABAergic signaling in the brain plays a critical role in general anesthesia (Franks, 2008; Mihic et al., 1997). Our results demonstrate that PD-1 regulates GABA

¹Center for Translational Pain Medicine, Department of Anesthesiology, Duke University Medical Center, Durham, NC 27710, USA

²Department of Neurobiology, Duke University Medical Center, Durham, NC 27710, USA

³Department of Cell Biology, Duke University Medical Center, Durham, NC 27710, USA

⁴Lead Contact

*Correspondence: ru-rong.ji@duke.edu

<https://doi.org/10.1016/j.isci.2020.101570>



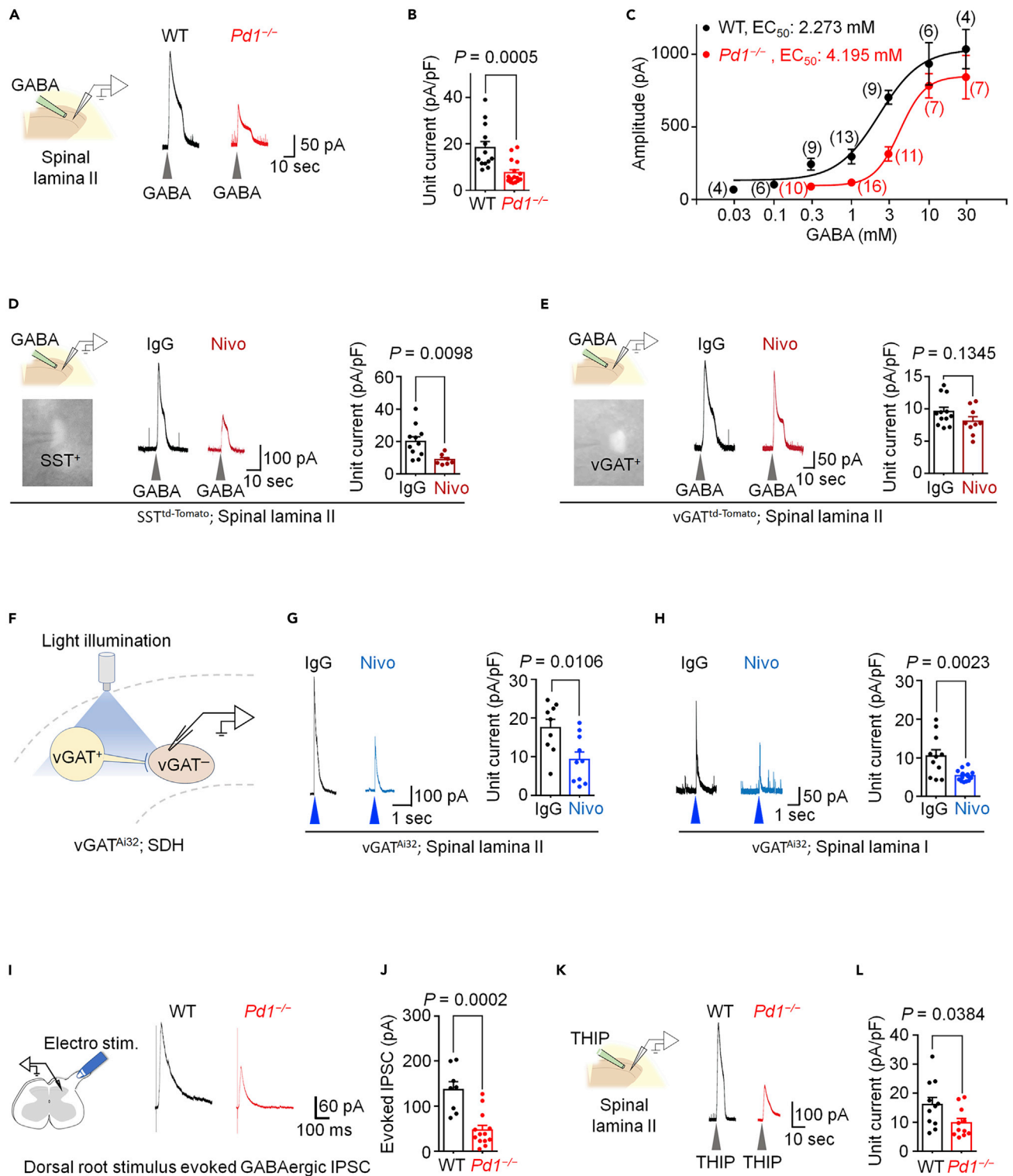


Figure 1. PD-1 is Required for GABAergic Signaling in SDH Neurons in Spinal Cord Slices

(A–C) GABA-induced currents in SDH lamina II neurons of WT and *Pd1^{-/-}* mice. (A) Left: experimental setup for local perfusion of GABA (1 mM) in spinal cord slices. Right: representative traces of currents evoked by transient GABA perfusion.

(B) Quantification of GABA-induced unit currents from WT and *Pd1^{-/-}* mice. n = 13 and 16 neurons from 4 animals.

Figure 1. Continued

(C) Dose-response curve plotting the average amplitude of GABA-induced currents. The curves were drawn according to the Hill equation. Values in parentheses denote the number of recorded neurons per group, each taken from 3–4 animals per group.

(D and E) GABA-induced currents in lamina II neurons of spinal cord slices from SST^{td-Tomato} reporter mice (D) and vGAT^{td-Tomato} reporter mice (E). Left top: experimental setup for GABA perfusion, as in (A). Left bottom: epifluorescence image of a spinal lamina II SST⁺ neuron or vGAT⁺ neuron with a recording pipette. Middle: traces of GABA (1 mM)-induced currents after incubation with IgG or Nivo (300 ng/mL, 2 h). Right: quantification of GABA-evoked unit currents. n = 11 (IgG, 6 mice, D); n = 7 (Nivo, 3 mice, D); n = 12 (IgG, 5 mice, E); n = 9 (Nivo, 4 mice, E).

(F–H) Blue-light-induced currents in spinal cord slices of vGAT^{Ai32} mice. (F) Schematic of experimental setup. vGAT⁺ neurons were stimulated with blue light (473 nm, 4 ms) to evoke endogenous GABA release, and postsynaptic currents were recorded from vGAT⁺ neurons in lamina II (G) and lamina I (H) neurons. (G) Left: representative traces of light-induced currents from vGAT⁺ neurons in spinal lamina II after incubation with IgG or Nivo (300 ng/mL, 2 h). Right: unit currents of light-evoked currents (n = 8 and 12 neurons from 3 animals/group). (H) Identical setup as in (G) but performed in spinal lamina I (n = 11 and 14 from 3 animals/group).

(I and J) Dorsal root stimulation evoked currents in spinal cord slices from WT and *Pd1*^{-/-} mice. (I) Left: experimental setup. An electrical stimulus was applied to the spinal dorsal root to evoke GABA-evoked IPSCs. Right: representative traces of evoked IPSCs from WT and *Pd1*^{-/-} mice. (J) Quantification of the amplitude of the evoked IPSCs from WT and *Pd1*^{-/-} mice. n = 8 and 13 neurons recorded from 4 and 3 animals, respectively.

(K–L) Same setup as in (A and B), but using the GABA_AR selective agonist THIP (1 mM; n = 11 neurons per group from 3 animals per group). Gray arrowheads indicate the application of GABA or THIP. Blue arrowheads indicate the blue light stimulus. V_H = 0 mV. Unpaired two-tailed t test. Each graph indicates the mean ± SEM.

receptor signaling in spinal and brain neurons and acts as an inhibitor of CNS neuronal activity. We also find that at the behavioral level, GABA-mediated analgesia and anesthesia were compromised in mice lacking *Pd1*.

RESULTS**Loss of PD-1 Function Impairs GABA-Mediated Currents in Dorsal Horn Neurons in Spinal Cord Slices**

To determine the role of PD-1 in regulating the function of GABAergic neurotransmission in the spinal dorsal horn (SDH), we prepared spinal cord slices and recorded GABA-evoked currents in outer lamina II (Ilo) neurons of wild-type (*Pd1*^{+/+}, WT) and *Pd1*^{-/-} (KO) mice (Figure 1A). Lamina Ilo interneurons are predominantly excitatory and form a nociceptive circuit with primary C-afferents and lamina I projection neurons (Braz et al., 2014; Duan et al., 2018; Todd, 2010). Local application of GABA (1 mM) to spinal cord slices of WT mice induced a robust outward current (Figure 1A), but this GABA-mediated current was markedly reduced in *Pd1*^{-/-} mice (Figure 1B). A dose-response curve analysis revealed a right-shift in *Pd1*-deficient neurons (WT: EC₅₀ = 2.3 mM, KO: EC₅₀ = 4.2 mM, Figure 1C).

Next we investigated whether impaired GABAergic neurotransmission in *Pd1*^{-/-} mice could be recapitulated by functional blockade of PD-1 in WT mice. Nivolumab is an anti-human PD-1 monoclonal antibody, clinically used as a cancer immunotherapeutic, which we previously reported also binds mouse PD-1 on mouse sensory neurons (Chen et al., 2017). We incubated spinal cord slices with Nivolumab or human IgG4 (an isotype control antibody) for 2 h at a low concentration (300 ng/mL ≈ 2.1 nM). These spinal cord slices were prepared from reporter mice that label somatostatin-expressing (SST⁺) excitatory neurons (Chamessian et al., 2018; Duan et al., 2014; Haring et al., 2018) or vGAT-expressing (vGAT⁺) inhibitory neurons (Figures 1D and 1E). Nivolumab markedly suppressed GABA-induced currents in lamina Ilo in SST⁺ neurons (Figure 1D), without altering GABA-induced currents in vGAT⁺ neurons (Figure 1E), suggesting that Nivolumab regulates GABAergic transmission primarily in excitatory neurons. We confirmed the GABA_A-mediated currents by complete blockade of the current by the selective antagonist bicuculline (Figure S1A).

To specifically activate inhibitory neurons in SDH, we employed an optogenetic approach using vGAT-Cre; Ai32 mice, wherein channelrhodopsin2 is expressed in inhibitory neurons. We activated inhibitory neurons by applying blue light stimulation onto spinal cord slices (Figure 1F). Blue light induced robust GABAergic outward currents (≈ 18 pA/pF) in lamina Ilo vGAT⁺ neurons, in the presence of strychnine (1 μM) during recordings (Figure 1G). Remarkably, Nivolumab treatment (2.1 nM, 2 h) suppressed the current by >50% in lamina Ilo neurons compared with immunoglobulin G (IgG) control (Figures 1F and 1G). As expected, this current was completely blocked by bicuculline (Figure S1B). Nivolumab also suppressed the blue-light-induced GABAergic currents in lamina I neurons (Figure 1H), supporting a broader effect of PD-1 in modulating inhibitory neurotransmission in SDH neurons. We further examined the paired-pulse ratio to assess the presynaptic modification by PD-1 in lamina Ilo neurons. We observed no difference in the ratio

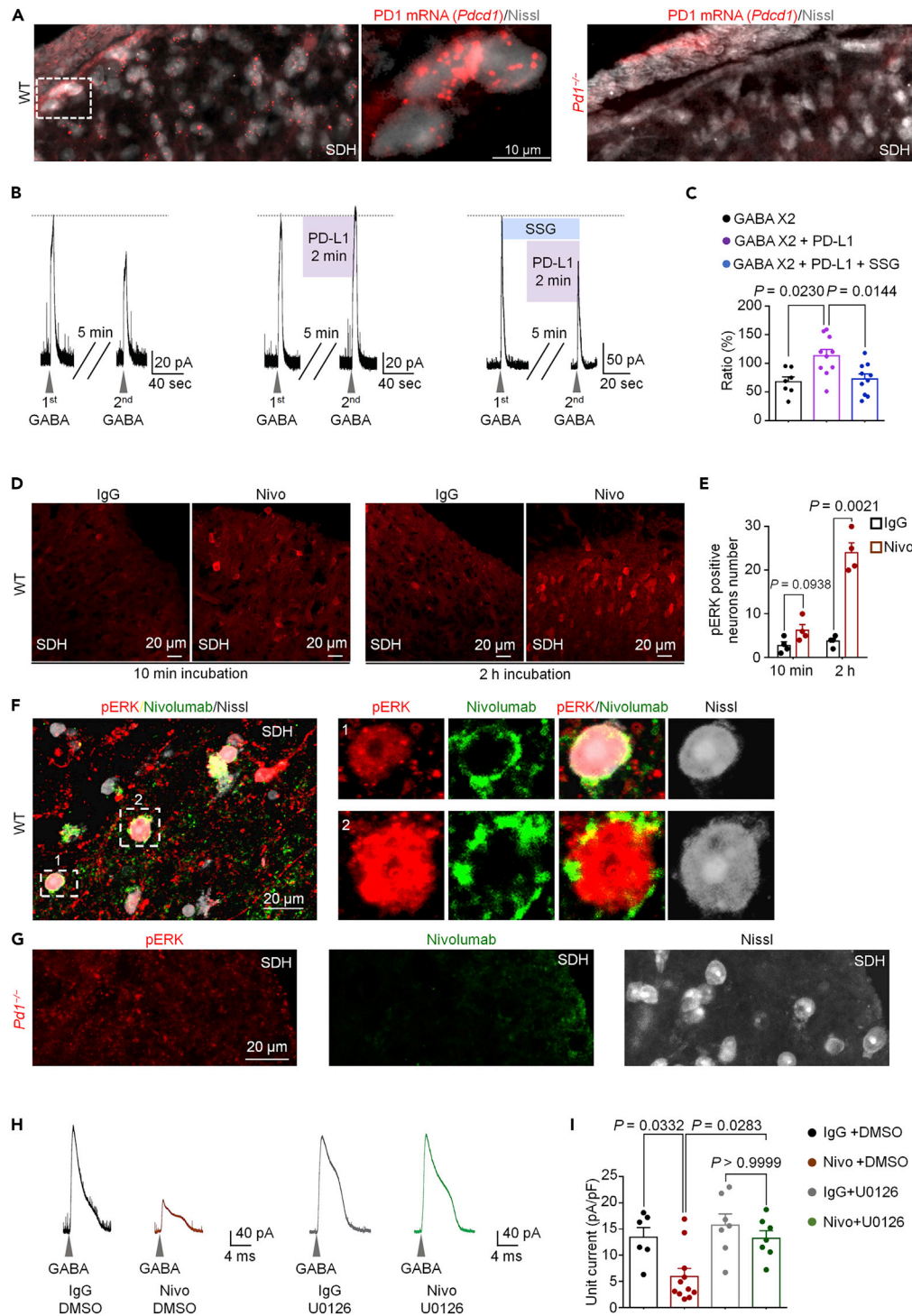


Figure 2. Nivolumab Binds PD-1 and Activates ERK to Suppress GABA Transmission in SDH Neurons

(A) Representative images showing localization of *Pd1* mRNA by fluorescent *in situ* hybridization in the superficial SDH in WT (left) and *Pd1*^{-/-} mice (right). Middle: higher magnification image of the dashed box. SDH neurons are labeled with Nissl staining. Note that *Pd1* mRNA expression is lost in *Pd1*^{-/-} mice (right).

(B) Left: representative currents induced by first GABA and second application of GABA (0.3 mM) in spinal lamina II neurons. Middle, same as left panel, but the second GABA application was combined with PD-L1 (30 ng/mL). Right: same as left panel, but the second GABA application was combined with PD-L1 and the SHP-1 inhibitor SSG (11 μM).

Figure 2. Continued

(C) Quantification of the amplitude of second GABA-induced currents (ratio of the first one) in vehicle/ACSF group (n = 8 neurons from 3 mice), PD-L1-treated group (n = 11 from 6 mice), and PD-L1- and SSG-treated group (n = 10 from 5 mice). (D–E) Nivolumab-induced pERK expression in spinal cord slices. (D) SDH immunostained for pERK following IgG or Nivo (300 ng/mL) incubation for 10 min (left) or 2 h (middle). (E) Quantification of the number of pERK-positive neurons in the SDH after IgG or Nivo incubation. n = 4 mice per group. (F and G) Left: double staining of pERK and Nivolumab in SDH from WT mice (F) and *Pd1*^{-/-} mice (G) after Nivo treatment (1000 ng/mL, 2 hr). Higher magnification images of box-1 and box-2 are indicated in the right panel in F, with each channel displayed separately. (H and I) Effects of U0126 on GABA-induced currents in lamina II neurons of spinal cord slices. (H) Example traces of GABA (1 mM)-induced currents after 2 h incubation with IgG and vehicle, Nivo (300 ng/mL) and vehicle, IgG and U0126 (1 μM), and Nivo (300 ng/mL), and U0126 (1 μM). (I) Unit currents of GABA currents after incubation with IgG and vehicle (n = 6 from 4 mice), Nivo and vehicle (n = 11 from 5 mice), IgG and U0126 (n = 7 from 3 mice), or Nivo and U0126 (n = 8 from 3 mice). Gray arrowheads indicate the application of GABA (1 mM). V_H = 0 mV. One-way ANOVA followed by Bonferroni post-hoc test. Data displayed indicate the mean ± SEM.

between Nivolumab and IgG-treated neurons (Figure S1C), indicating a postsynaptic modification of inhibitory synaptic transmission by PD-1.

We next recorded evoked synaptic GABA currents in SDH by electrical stimulation of the dorsal root attached to a spinal cord slice (Figure 1I). The evoked GABA inhibitory postsynaptic currents (IPSCs) were significantly reduced in lamina II neurons of KO mice (p = 0.0002, versus WT, Figures 1I and 1J). $\alpha 1$ and $\alpha 2$ are two major subunits of GABA_A receptors in SDH (Zeilhofer et al., 2012), and $\alpha 2$ subunit is the predominant one in the superficial layers of SDH (Paul et al., 2012). Western blot analysis showed comparable expression of $\alpha 1$ and $\alpha 2$ subunits in SDH of WT and KO mice (Figure S1E).

We also found that GABA-current in the SDH was mediated by inotropic GABA_A receptor, as the GABA_A antagonist completely blocked the current (Figures S1A). Local application of the GABA_A agonist THIP (1 mM) elicited a robust outward current of ~16.5 pA/pF in lamina II neurons, but this GABA_A-mediated current was substantially reduced in neurons lacking *Pd1* (Figures 1K–1L), showing a 5-fold change in EC₅₀ values (WT: 0.17 mM; KO: 0.87 mM; Figure S1D). Thus, PD-1 regulates GABAergic transmission via GABA_A receptors in spinal cord neurons.

Nivolumab Binds PD-1 and Activates ERK to Suppress GABA Transmission in SDH Neurons

We investigated *Pd1* mRNA and PD-1 protein expression in SDH neurons using *in situ* hybridization and immunohistochemistry. *In situ* hybridization with RNAscope revealed *Pd1* mRNA expression in SDH neurons of WT mice but not *Pd1*^{-/-} mice (Figure 2A). Immunohistochemistry showed broad expression of PD-1 in SDH neurons, including laminae I and II neurons, and this expression was abolished by blocking peptide treatment in WT mice and in *Pd1*^{-/-} mice (Figures S2A). We also observed that approximately 70% of excitatory neurons and 40% of inhibitory neurons in SDH express *Pd1* mRNA, supporting a primary modulation of excitatory neuron function by PD-1 (Figures S2B and S2C).

Neurokinin-1 receptor (NK1R, encoded by *Tacr1*) is expressed by projection neurons in the spinal lamina I (Ikeda et al., 2003; Todd, 2010), and NK1R + projection neurons exhibit marked synaptic plasticity following tissue injury and are essential for generating pathological pain (Ikeda et al., 2003; Mantyh et al., 1997; Nichols et al., 1999). Interestingly, *Pd1* was expressed by 80% of *Tacr1*+ neurons, in further support of its role of regulating the function of these key projection neurons (Figures S2D and S2E). *Pd1* transcript was absent in SDH of *Pd1*^{-/-} mice (Figure S2F).

PD-L1 and PD-L2 are endogenous ligands of PD-1, and administration of PD-L1 was shown to suppress pain via PD-1 and a downstream tyrosine phosphatase SHP-1 (Chen et al., 2017). We observed that PD-1 activation by PD-L1 (30 ng/mL) enhanced GABA (0.3 mM)-induced current in SDH neurons (Figures 2B and 2C). Application of the SHP-1 inhibitor SSG (Chen et al., 2017) blocked the effect of PD-L1 in SDH neurons (Figures 2B and 2C), suggesting an involvement of SHP-1 in PD-1 modulation of GABA transmission. *In situ* hybridization revealed very low expression of *Pd1* mRNA (*CD274*) and *Pd2* (*CD273*) mRNA in SDH (Figure S2I). However, *Pd1* was previously detected in DRG neurons, and PD-L1 protein was also detected in DRG and spinal cord tissues by ELISA (Chen et al., 2017). It is likely that PD-1 in SDH could be activated by PD-L1 released from primary sensory neurons.

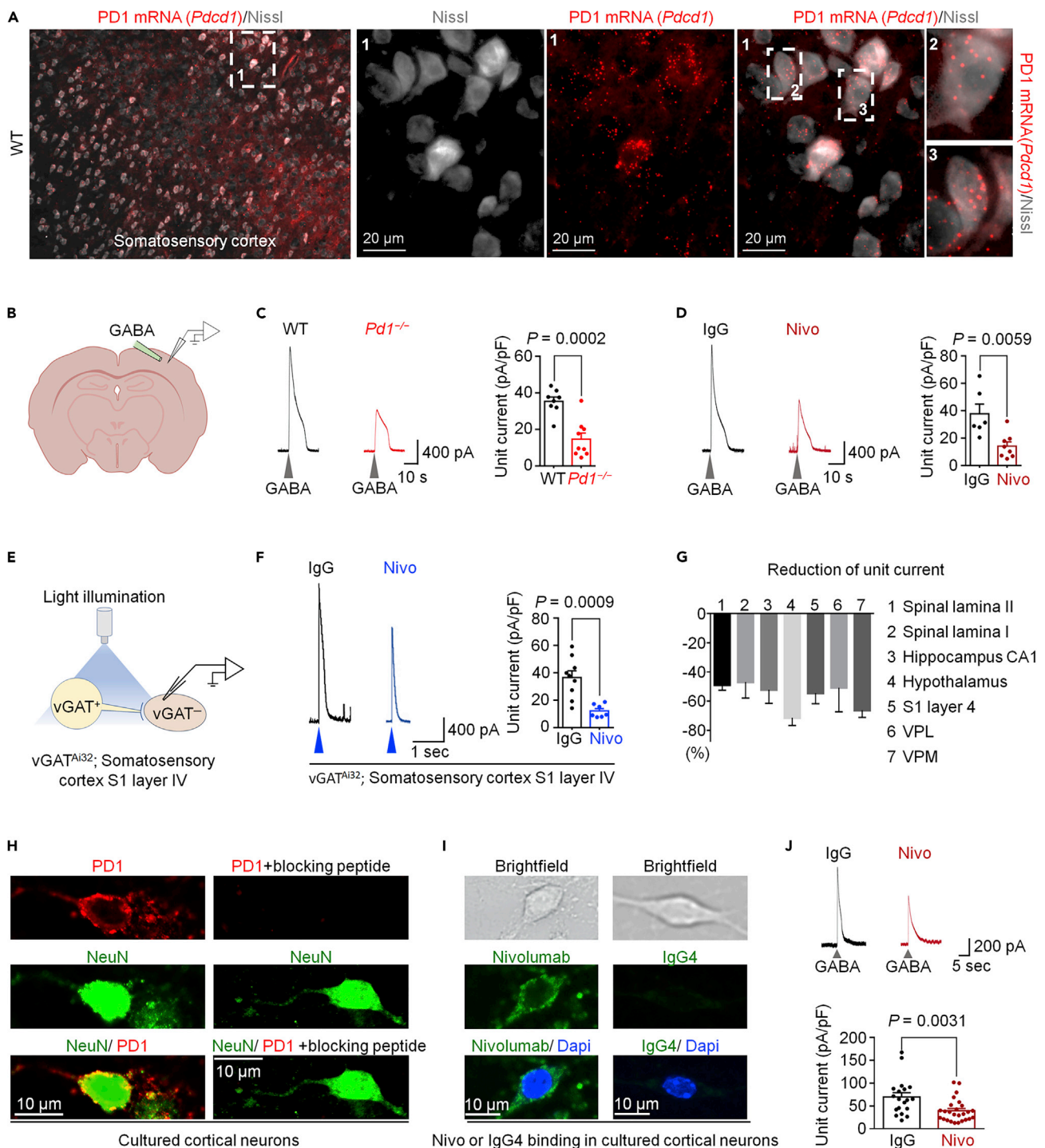


Figure 3. PD-1 Modulates GABA-Mediated Currents in Brain Slices and Dissociated Cortical Neurons

(A) Left: *in situ* hybridization for *Pd1* mRNA expression on somatosensory cortical neurons (co-stained with Nissl in gray) in WT mice. The box is enlarged in three middle panels (labeled with 1). Boxes 2 and 3 are enlarged on the right panels.

(B–D) GABA-induced currents in S1 cortex of brain slices. (B) Experimental setup used for local perfusion of GABA in the layer IV of somatosensory cortex. (C) Left: exemplary traces of currents irritated by transient GABA (1 mM) perfusion from WT and *Pd1*^{-/-} mice. Right: unit currents. n = 8 and 9 from 3 animals/group. (D) Left: exemplary traces of currents produced by GABA (1 mM) perfusion after incubation with IgG or Nivo (300 ng/mL, 2 h). Right: unit currents. n = 6 and 8 from 5 and 3 animals, respectively.

Figure 3. Continued

(E–G) Light-evoked GABA currents in brain slices produced from vGAT^{Ai32} mice. (E) Experimental setup showing vGAT⁺ neurons stimulated with blue light (473 nm, 4 ms) and postsynaptic current recorded from vGAT-negative neurons in the layer IV of somatosensory cortex. (F) Left: exemplary traces of light-induced currents from vGAT-negative neurons treated with IgG or Nivo (300 ng/mL, 2 h). Right: unit currents of light-induced currents. n = 9 and 8, from 3 animals/group. (G) Percentile reduction of light-induced unit currents by Nivolumab (300 ng/mL, 2 h) in different regions of spinal cord and brain. (H–J) Inhibition of GABA-induced currents by Nivolumab in cultured cortical neurons. (H) Left: double staining of PD-1 and NeuN in cultured cortical neurons. Right: absence of PD-1 immunostaining upon treatment of a blocking peptide. (I) Top: bright field images of cultured cortical neurons. Middle and bottom: immunostaining for Nivo or IgG4 after Nivo or IgG4 (300 ng/mL, 2 h). (J) Upper: exemplary traces of GABA (1 mM)-induced currents in cortical neurons treated with IgG or Nivo (300 ng/mL, 2 h). Lower: unit currents of GABA currents. n = 19 and 26 from 3 animals per group. The cortical neurons were cultured for 7–8 days before experiment. Gray arrowheads indicate the application of GABA. Blue arrowheads indicate the illumination of blue light. V_H = 0 mV. Unpaired two-tailed t test. All error bars indicate the mean ± SEM.

SHP-1 is known to suppress the activation (phosphorylation) of extracellular signaling-regulated kinase (pERK) in immune cells (Cerny et al., 2017). Phosphorylation of extracellular signaling-regulated kinase (pERK) in SDH neurons following intense noxious stimulation or tissue injury plays an important role in neuronal sensitization and pain hypersensitivity (Ji et al., 2009; Karim et al., 2001). Strikingly, incubation of spinal cord slices with Nivolumab for 2 h, in the absence of PD-L1 or nociceptive stimuli, was sufficient to induce pERK expression in SDH neurons (Figures 2D and 2E). Double staining revealed many SDH neurons showing both Nivolumab labeling (green) and pERK expression (red) after the Nivolumab treatment (Figure 2F). This double labeling was abolished in spinal sections of *Pd1*^{-/-} mice (Figure 2G). These data suggest that (1) Nivolumab binds to SDH neurons in a PD-1-dependent manner and (2) Nivolumab binding is associated with pERK induction. We also found that the majority of pERK-labeled neurons were SST⁺ excitatory neurons (Figures S2G and S2H). To assess the functional contribution of ERK, we treated spinal cord slices with an ERK kinase inhibitor U0126 (1 μM), given 20 min prior to patch recording. We observed that the Nivolumab-induced inhibition of GABA currents was blocked by U0126 (Figures 2H and 2I). Collectively, these results indicate that (1) there is a constitutive activity of PD-1 in the absence of its ligands and (2) Nivolumab activates ERK to suppress GABAergic transmission in SDH neurons.

PD-1 Modulates GABA-Mediated Currents in Different Brain Regions

In situ hybridization and immunohistochemistry showed broad expression of *Pd1* mRNA and PD-1 protein in S1 somatosensory cortex (Figures 3A and S3A). We prepared brain slices for patch clamp recordings in layer IV vGAT-negative neurons of S1 cortex in WT and *Pd1*^{-/-} mice, as well as WT mice treated with Nivolumab (Figure 3B). We observed a substantial reduction of GABA-induced currents in KO mice (compared with WT mice, Figure 3C) and also in WT-S1 neurons treated with Nivolumab (compared with IgG, Figure 3D). Furthermore, in the presence of strychnine, blue-light-evoked GABAergic currents in S1-layer IV neurons was suppressed by Nivolumab (Figures 3E and 3F). Nivolumab had no effect on GABA-induced currents in S1-vGAT⁺ neurons (Figure S3B), suggesting that PD-1 might modulate GABA-currents selectively in excitatory cortical neurons.

We also tested the actions of Nivolumab on blue-light-evoked GABAergic currents in neurons of the brain regions in the thalamus that are involved in pain modulation, including the ventrolateral thalamic nucleus (VPL) and ventromedial thalamic nucleus (VPM), both of which expressed PD-1 (Figure S3C). We observed a marked reduction of the light-evoked GABA currents in vGAT⁻ neurons in the VPL and VPM by Nivolumab (Figures 3G and S3D–S3E), but no difference was observed in vGAT⁺ neurons in the thalamus. Compared with IgG, Nivolumab also suppressed light-induced GABA currents in vGAT⁻ neurons in hippocampal CA1 and hypothalamic neurons (Figures 3G and S3G–S3H). The reduction of GABA currents in different brain regions ranged from 50%–70% (Figure 3G). Compared with the spinal cord, the distribution of the GABA_A receptor subunits in the brain is more sophisticated, but the α1 subunit is the most abundant one in almost all the regions (Pirker et al., 2000; Sieghart et al., 1999). Western blotting showed comparable expression of α1 subunit of GABA_A receptor in the somatosensory cortex, thalamus, and hypothalamus in WT and KO mice (Figures S2I–S2J). Together, these results suggest that PD-1 is a pan-neuronal modulator of GABAergic transmission in the CNS, without affecting the expression of GABA_A receptor.

Spinal cord and brain slices contain non-neuronal cells such as immune cells and glial cells that may also express PD-1 to regulate neuronal activities indirectly. To this end, we assessed a direct role of PD-1 in regulating GABA transmission in dissociated cortical neurons. We observed PD-1 expression on primary cultures of cortical neurons of WT but not KO mice at 7–8 days in culture (DIV 7–8, Figure 3H). Nivolumab, but not IgG, was able to bind on cultured cortical neurons (Figure 3I). GABA application (1 mM) induced a

large outward current in dissociated neurons, but this GABA current was reduced by Nivolumab treatment (300 ng/mL, 2 h, [Figure 3J](#)). Thus, inhibition of PD-1 in cortical neurons may be sufficient to alter GABA signaling.

Loss of PD-1 Results in Deficits in GABA-Mediated Analgesia and Anesthesia in Mice

GABAergic signaling in SDH plays a critical role in pain control ([Coull et al., 2005](#); [Knabl et al., 2008](#); [Lu et al., 2013](#); [Zeilhofer et al., 2012](#)). We assessed whether GABA_A-mediated analgesia would require PD-1 signaling. Intrathecal administration of GABA_A agonist THIP (3 nmol) produced a transient reversal of inflammatory pain induced by Complete Freund's adjuvant (CFA) in WT mice. Remarkably, this reversal of mechanical allodynia was compromised in *Pd1*^{-/-} mice ([Figure 4A](#)), as well as in WT mice treated with intrathecal Nivolumab (1 μg, [Figure 4B](#)). In addition, intrathecal administration of a lower concentration of THIP (1 nmol) transiently reduced CFA-induced inflammatory pain and nerve-injury-induced neuropathic pain (mechanical allodynia), which was also impaired by Nivolumab ([Figures S4A–S4B](#)). Thus, PD-1 plays an active role in GABA_A-mediated analgesia.

General anesthesia requires GABAergic signaling in multiple brain regions including the thalamus and hypothalamus ([Franks, 2008](#); [Mihic et al., 1997](#)). We investigated isoflurane-induced general anesthesia using a gas monitor in WT and *Pd1*^{-/-} mice ([Figure 4C](#)). A dose-response analysis revealed a right shift in the concentration of isoflurane (WT: EC₅₀ = 0.8425%; KO: EC₅₀ = 0.9820%; [Figure 4D](#)). The induction time of anesthesia (loss of turnover response) at 2%, 2.5%, and 3% isoflurane were all significantly increased in KO mice ($p < 0.01$, [Figure 4E](#)). In contrast, the emergence time (recovery phase) was not altered in KO mice ([Figure 4E](#)). This result could be expected, as the emergence mechanisms of general anesthesia are different from that of induction ([Franks, 2008](#)). We also evaluated the effects of Nivolumab on 1.5% isoflurane-induced general anesthesia following intracerebroventricular (ICV) injection ([Figure S4C](#)) of IgG or Nivolumab (3 μg in 5 μL) 1 h prior to assessment. We did not observe significant changes in induction and emergence time between IgG- and Nivolumab-treated mice, but observed a trend toward increase in the induction time and decrease in the emergence time ([Figure S4C](#)). The injectable anesthetic pentobarbital also binds to GABA_AR, and this interaction plays an important role in the anesthetic action ([Franks, 2008](#)). Notably, the induction time of anesthesia by pentobarbital (40 mg/kg, i.p.) was prolonged in *Pd1*^{-/-} mice ([Figure 4F](#)). Thus, these data provide evidence at the behavioral level that PD-1 regulates GABAergic neurotransmission by regulating the effects of multiple GABA_AR-mediated types of anesthesia.

DISCUSSION

Our study has revealed a previously unrecognized modulation of GABAergic neurotransmission by PD-1, a leading molecular target of cancer immunotherapy. We found that PD-1 blockade with Nivolumab caused a profound reduction (45%–70%) of GABA-currents across the CNS, including lamina I and lamina II neurons in SDH, S1 cortical neurons, thalamic neurons in the VPM and VPL, hypothalamic neurons, and hippocampal neurons ([Figure 3G](#)). Furthermore, spinal cord and cortical neurons of *Pd1*^{-/-} mice showed the same degree of reduction in GABA currents (45%–60%, [Figure 3G](#)) compared with WT neurons. At behavioral levels, GABA-mediated analgesia and anesthesia were impaired in *Pd1*^{-/-} mice. Furthermore, Nivolumab exhibited binding to SDH and cortical neurons and inhibited GABA currents in dissociated cortical neurons from primary cultures, providing evidence of possible direct action on neurons.

We propose that PD-1 regulates GABA_A signaling via SHP-1 and ERK signaling ([Figure S4D](#)). Given that GABA_A-mediated currents and analgesia were compromised in KO mice and the expression of $\alpha 1$ and $\alpha 2$ subunits of GABA_A did not change in KO mice, PD-1 may interact with GABA_A to regulate GABAergic signaling. The phosphatase SHP-1/2 is involved in downstream signaling of PD-1 in immune cells and DRG neurons ([Chen et al., 2017](#); [Hebeisen et al., 2013](#)). This involvement was also demonstrated in SDH neurons ([Figure 2C](#)). It is conceivable that PD-1 regulates the activity of GABA_A through SHP-1 signaling. Although PD-1 inhibition reduced GABA current, PD-1 activation by PD-L1 enhanced GABA current in SDH neurons in an SHP-dependent manner. Strikingly, Nivolumab treatment was sufficient to activate ERK in SDH neurons, in the absence of additional stimuli. Nivolumab-induced suppression of GABA currents was blocked by the ERK inhibitor U0126, providing a link between Nivolumab, ERK, and GABA transmission ([Figure S4D](#)). It is noteworthy that ERK was also implicated as a negative regulator of GABA_A function via an ERK phosphorylation site ([Bell-Horner et al., 2006](#)).

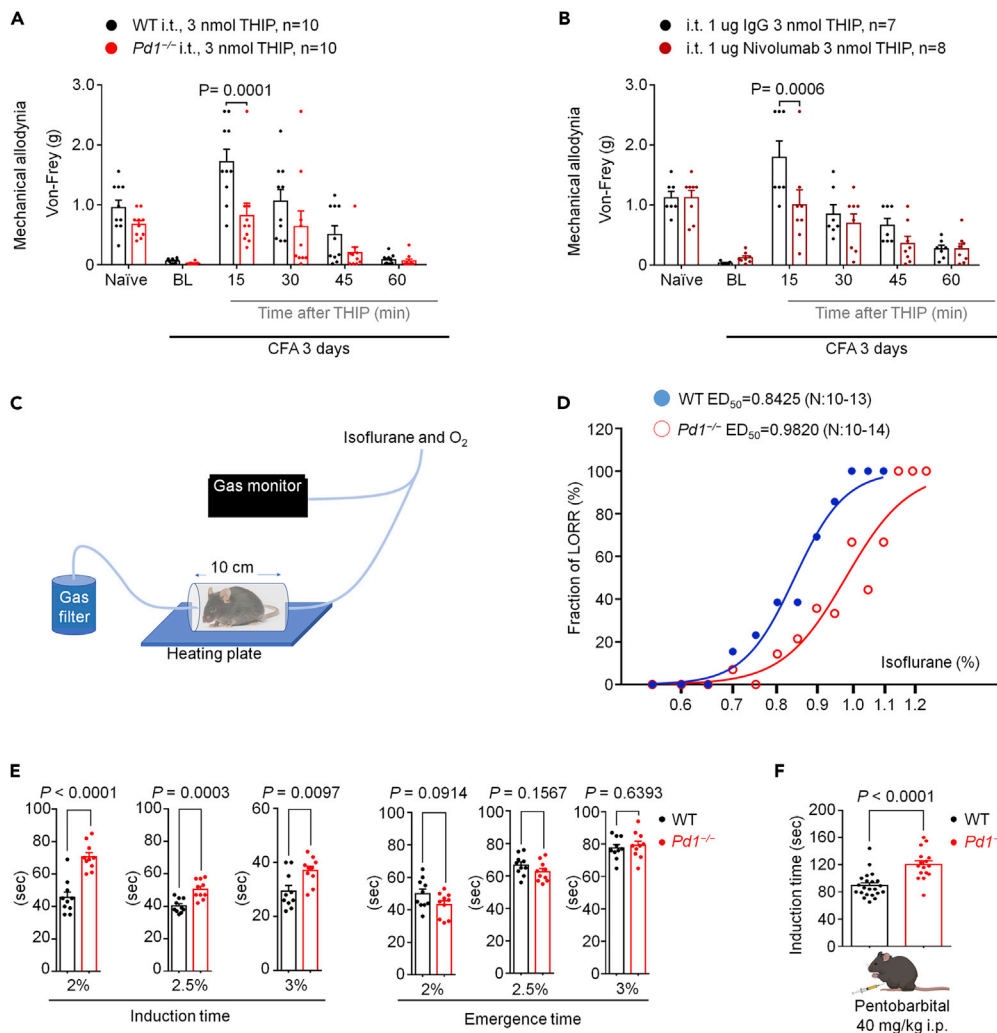


Figure 4. GABA_AR-Mediated Antinociception and Anesthesia is Impaired in *Pd1*^{-/-} Mice

(A and B) GABA_AR-mediated antinociception in WT and *Pd1*^{-/-} mice. (A) von Frey testing showing the effect of intrathecal THIP (3 nmol) on CFA-induced inflammatory pain. $p = 0.0001$, WT versus *Pd1*^{-/-}, two-way ANOVA, followed by Bonferroni's post hoc test. (B) von Frey testing showing the effect of intrathecal THIP (3 nmol) on CFA-induced inflammatory pain in mice pretreated with IgG4 or nivolumab (1 µg, i.t.). $p = 0.0006$, IgG4 + THIP versus nivolumab + THIP, two-way ANOVA, followed by Bonferroni's post-hoc test.

(C–F) GABA_AR-mediated anesthesia in WT and *Pd1*^{-/-} mice. (C) Experimental setup used to assess isoflurane anesthesia-mediated loss of righting reflex (LORR). (D) Dose-response curves of the fraction of LORR in WT or *Pd1*^{-/-} mice at various concentrations of isoflurane. The curves were drawn according to the Hill equation. (E) The effects of different doses of isoflurane on induction and emergence time in WT or *Pd1*^{-/-} mice ($n = 10$ animals in each group). Unpaired two-tailed t test. (F) The effects of sodium pentobarbital on anesthesia induction time in WT or *Pd1*^{-/-} mice ($n = 22$ and 16 animals). Unpaired two-tailed t test.

All error bars indicate the mean ± SEM.

Our *in situ* hybridization and immunohistochemistry data demonstrated a broad expression of PD-1 and *Pd1* mRNA in neurons across different CNS regions. However, single-cell analysis suggested low expression levels of *Pd1* mRNA in excitatory cortical neurons (Zeisel et al., 2018). This discrepancy may be due to the low sensitivity of single-cell RNA-sequencing approaches, where only the 10%–20% most highly expressed mRNAs are typically detected. Nevertheless, neuronal PD-1 expression is functional in multiple spinal cord and brain regions (Figure 3G). We cannot rule out the possibility that non-neuronal cells also contribute to the neuronal changes we saw in spinal cord and brain slices after PD-1 blockade, as inhibition of PD-1 could enhance microglia activation in SDH (Wang et al., 2020b). However, dissociated cortical

neurons in culture clearly displayed binding to Nivolumab (Figure 3I), and furthermore, Nivolumab was sufficient to suppress GABA-induced currents in these dissociated neurons in cultures (Figure 3J).

Our findings suggest that immunotherapy via Nivolumab and other anti-PD1 therapeutics could impair GABA-mediated analgesia, which is consistent with reduced GABA-analgesia in *Pd1*^{-/-} mice lacking *Pd1*. “Gate control,” an important theory for pain regulation, is mediated by GABAergic transmission in SDH, and loss of GABAergic transmission, a cardinal feature of chronic pain such as neuropathic pain, would open the gate for the pathogenesis of pain (Braz et al., 2014; Duan et al., 2018; Lu et al., 2013; Melzack and Wall, 1965; Moore et al., 2002). On the other hand, it has been shown that spinal transplantation of GABA-precursor neurons could effectively control neuropathic pain (Braz et al., 2012). Notably, our previous studies demonstrated that loss of PD-1 resulted in increased basal pain sensitivity (Chen et al., 2017; Wang et al., 2020a, 2020b), which may mimic a chronic pain condition due to impaired GABAergic transmission in SDH neurons.

An anesthesiologist in the lab initially noticed difficulty to anesthetize the *Pd1*^{-/-} mice during surgery. Further quantitative analysis revealed an increase in the induction time but no change in the emergence time (Figure 4E). However, ICV administration of Nivolumab did not significantly change the induction and emergence time. It is possible that only limited brain regions are affected by ICV administration, and it requires PD-1 modulation of GABA transmission in multiple brain regions to alter anesthesia. Regarding typical nervous system side effects such as fatigue, headache, dysgeusia, vertigo and anxiety or malaise, Nivolumab is relatively safe (Kwatra et al., 2018). However, neurological issues have been reported, such as polyneuropathy and encephalopathy (Mirabile et al., 2019). We should also point out that half-life of Nivolumab in mouse is much shorter than that in human (3 days versus weeks) (Wang et al., 2020a). One systematic review found that benefits were observed with PD-1 blockade in melanomas with metastasis to the brain, and Nivolumab concentrations could reach from 35 to 150 ng/mL in CSF of these patients (van Bussel et al., 2019). As tested in this study, this concentration range may be sufficient to affect neuronal activities. Future studies are warranted to investigate the neurological effects of anti-PD-1 therapies in patients in whom significant CNS penetration of antibody has occurred after brain injury.

In summary, we have identified PD-1 as a pan-neuronal modulator of GABA receptor signaling. In particular, PD-1 is an essential signaling component for the function of GABA_A across different CNS regions in the spinal cord and brain. Thus, PD-1 may act as an inhibitor for neurons as well as for immune cells. Clinical application of PD-1 inhibitors may produce beneficial effects in some disease conditions by enhancing neuronal activities, thus representing a potential neurotherapy, or may produce its beneficial actions through a combination of actions on immune cells and neurons (immunotherapy and neurotherapy).

Limitations of the Study

There are several unresolved issues in this study. First, the most direct evidence for PD-1 operating in neurons is from cultured embryonic cortical neurons, which may contain possible contamination of glial cells. Future studies are warranted to conditionally delete *Pd1* selectively in neurons, glial cells, and immune cells to test the respective contribution of PD-1 in each cell type to GABAergic signaling using conditional *Pd1* knockout mice. Second, the source of PD-1 ligands (e.g., PD-L1 and PD-L2) in the spinal cord remains to be identified. Because primary sensory neurons express PD-L1 (Chen et al., 2017), PD-1 could be activated by PD-L1 released from the central terminals of primary afferents in the spinal cord. We also do not rule out the possibility that PD-1 may signal in a ligand-independent manner. Additionally, we focus on spinal α 1 and α 2 subunits of GABA_A receptors in this study, but the contribution of β and γ subunits in PD-1-mediated regulation of GABAergic transmission should also be considered in future studies. Finally, it is important to note that many basic discoveries in animals fail to translate to humans. Future clinical studies which carefully monitor anesthesia induction time on patients receiving anti-PD1 therapies are warranted to determine the clinical ramifications of these findings.

Resource Availability

Lead Contact

Ru-Rong Ji, ru-rong.ji@duke.edu.

Materials Availability

All the materials are commercially available.

Data and Code Availability

Available upon request.

METHODS

All methods can be found in the accompanying [Transparent Methods supplemental file](#).

SUPPLEMENTAL INFORMATION

Supplemental Information can be found online at <https://doi.org/10.1016/j.isci.2020.101570>.

ACKNOWLEDGMENTS

This study was supported by Duke University Anesthesiology Research Funds.

AUTHOR CONTRIBUTIONS

C.J. and R.R.J developed the project. C.J., Z.W., C.R.D., K.W., A.S.A., X.T.M.M. and J.Z. conducted experiments; R.R.J. and C.J. wrote the manuscript. C.R.D. edited the manuscript.

DECLARATION OF INTERESTS

Dr. Ji is a consultant of Boston Scientific and serves on Scientific Advisory Board of Alleviate Therapeutics. These activities are not related to this study. Drs. Ji, Jiang, and Wang also filed a patent “Methods and kits for treating pain” (16/612,909) from Duke University, which is related to this study.

Received: July 1, 2020

Revised: September 1, 2020

Accepted: September 14, 2020

Published: October 23, 2020

REFERENCES

- Baruch, K., Deczkowska, A., Rosenzweig, N., Tsitsou-Kampeli, A., Sharif, A.M., Matcovitch-Natan, O., Kertser, A., David, E., Amit, I., and Schwartz, M. (2016). PD-1 immune checkpoint blockade reduces pathology and improves memory in mouse models of Alzheimer’s disease. *Nat. Med.* 22, 135–137.
- Bell-Horner, C.L., Dohi, A., Nguyen, Q., Dillon, G.H., and Singh, M. (2006). ERK/MAPK pathway regulates GABAA receptors. *J. Neurobiol.* 66, 1467–1474.
- Brahmer, J.R., Tykodi, S.S., Chow, L.Q., Hwu, W.J., Topalian, S.L., Hwu, P., Drake, C.G., Camacho, L.H., Kauh, J., Odunsi, K., et al. (2012). Safety and activity of anti-PD-L1 antibody in patients with advanced cancer. *N Engl. J. Med.* 366, 2455–2465.
- Braz, J., Solorzano, C., Wang, X., and Basbaum, A.I. (2014). Transmitting pain and itch messages: a contemporary view of the spinal cord circuits that generate gate control. *Neuron* 82, 522–536.
- Braz, J.M., Sharif-Naeini, R., Vogt, D., Kriegstein, A., Alvarez-Buylla, A., Rubenstein, J.L., and Basbaum, A.I. (2012). Forebrain GABAergic neuron precursors integrate into adult spinal cord and reduce injury-induced neuropathic pain. *Neuron* 74, 663–675.
- Cerny, O., Anderson, K.E., Stephens, L.R., Hawkins, P.T., and Sebo, P. (2017). cAMP signaling of adenylate cyclase toxin blocks the oxidative burst of neutrophils through epac-mediated inhibition of phospholipase C activity. *J. Immunol.* 198, 1285–1296.
- Chamessian, A., Young, M., Qadri, Y., Berta, T., Ji, R.R., and Van de Ven, T. (2018). Transcriptional profiling of somatostatin interneurons in the spinal dorsal horn. *Sci. Rep.* 8, 6809.
- Chen, G., Kim, Y.H., Li, H., Luo, H., Liu, D.L., Zhang, Z.J., Lay, M., Chang, W., Zhang, Y.Q., and Ji, R.R. (2017). PD-L1 inhibits acute and chronic pain by suppressing nociceptive neuron activity via PD-1. *Nat. Neurosci.* 20, 917–926.
- Chiu, I.M., von Hehn, C.A., and Woolf, C.J. (2012). Neurogenic inflammation and the peripheral nervous system in host defense and immunopathology. *Nat. Neurosci.* 15, 1063–1067.
- Coull, J.A., Beggs, S., Boudreau, D., Boivin, D., Tsuda, M., Inoue, K., Gravel, C., Salter, M.W., and De Koninck, Y. (2005). BDNF from microglia causes the shift in neuronal anion gradient underlying neuropathic pain. *Nature* 438, 1017–1021.
- Dong, H., Zhu, G., Tamada, K., and Chen, L. (1999). B7-H1, a third member of the B7 family, co-stimulates T-cell proliferation and interleukin-10 secretion. *Nat. Med.* 5, 1365–1369.
- Donnelly, C.R., Chen, O., and Ji, R.R. (2020). How do sensory neurons sense danger signals? *Trends Neurosci.* S0166-2236(20)30173-30179.
- Duan, B., Cheng, L., Bourane, S., Britz, O., Padilla, C., Garcia-Campmany, L., Krashes, M., Knowlton, W., Velasquez, T., Ren, X., et al. (2014). Identification of spinal circuits transmitting and gating mechanical pain. *Cell* 159, 1417–1432.
- Duan, B., Cheng, L., and Ma, Q. (2018). Spinal circuits transmitting mechanical pain and itch. *Neurosci. Bull.* 34, 186–193.
- Franks, N.P. (2008). General anaesthesia: from molecular targets to neuronal pathways of sleep and arousal. *Nat. Rev. Neurosci.* 9, 370–386.
- Freeman, G.J., Long, A.J., Iwai, Y., Bourque, K., Chernova, T., Nishimura, H., Fitz, L.J., Malenkovich, N., Okazaki, T., Byrne, M.C., et al. (2000). Engagement of the PD-1 immunoinhibitory receptor by a novel B7 family member leads to negative regulation of lymphocyte activation. *J. Exp. Med.* 192, 1027–1034.
- Haring, M., Zeisel, A., Hochgerner, H., Rinwa, P., Jakobsson, J.E.T., Lonnerberg, P., La Manno, G., Sharma, N., Borgius, L., Kiehn, O., et al. (2018). Neuronal atlas of the dorsal horn defines its architecture and links sensory input to transcriptional cell types. *Nat. Neurosci.* 21, 869–880.
- Hebeisen, M., Baitsch, L., Presotto, D., Baumgaertner, P., Romero, P., Michielin, O., Speiser, D.E., and Rufer, N. (2013). SHP-1 phosphatase activity counteracts increased T cell receptor affinity. *J. Clin. Invest.* 123, 1044–1056.
- Herbst, R.S., Soria, J.C., Kowanetz, M., Fine, G.D., Hamid, O., Gordon, M.S., Sosman, J.A.,

- McDermott, D.F., Powderly, J.D., Gettinger, S.N., et al. (2014). Predictive correlates of response to the anti-PD-L1 antibody MPDL3280A in cancer patients. *Nature* 515, 563–567.
- Ikeda, H., Heinke, B., Ruscheweyh, R., and Sandkuhler, J. (2003). Synaptic plasticity in spinal lamina I projection neurons that mediate hyperalgesia. *Science* 299, 1237–1240.
- Ishida, Y., Agata, Y., Shibahara, K., and Honjo, T. (1992). Induced expression of PD-1, a novel member of the immunoglobulin gene superfamily, upon programmed cell death. *EMBO J.* 11, 3887–3895.
- Ji, R.R., Gereau, R.W., Malcangio, M., and Strichartz, G.R. (2009). MAP kinase and pain. *Brain Res. Rev.* 60, 135–148.
- Karim, F., Wang, C.C., and Gereau, R.W. (2001). Metabotropic glutamate receptor subtypes 1 and 5 are activators of extracellular signal-regulated kinase signaling required for inflammatory pain in mice. *J. Neurosci.* 21, 3771–3779.
- Knabl, J., Witschi, R., Hosl, K., Reinold, H., Zeilhofer, U.B., Ahmadi, S., Brockhaus, J., Sergejeva, M., Hess, A., Brune, K., et al. (2008). Reversal of pathological pain through specific spinal GABAA receptor subtypes. *Nature* 451, 330–334.
- Kwatra, S.G., Stander, S., and Kang, H. (2018). PD-1 blockade-induced pruritus treated with a mu-opioid receptor antagonist. *N. Engl. J. Med.* 379, 1578–1579.
- Latta-Mahieu, M., Elmer, B., Bretteville, A., Wang, Y., Lopez-Grancha, M., Goniot, P., Moindrot, N., Ferrari, P., Blanc, V., Schussler, N., et al. (2018). Systemic immune-checkpoint blockade with anti-PD1 antibodies does not alter cerebral amyloid-beta burden in several amyloid transgenic mouse models. *Glia* 66, 492–504.
- Liu, T., Xu, Z.Z., Park, C.K., Berta, T., and Ji, R.R. (2010). Toll-like receptor 7 mediates pruritus. *Nat. Neurosci.* 13, 1460–1462.
- Lu, Y., Dong, H., Gao, Y., Gong, Y., Ren, Y., Gu, N., Zhou, S., Xia, N., Sun, Y.Y., Ji, R.R., et al. (2013). A feed-forward spinal cord glycinergic neural circuit gates mechanical allodynia. *J. Clin. Invest.* 123, 4050–4062.
- Mantyh, P.W., Rogers, S.D., Honore, P., Allen, B.J., Ghilardi, J.R., Li, J., Daughters, R.S., Lappi, D.A., Wiley, R.G., and Simone, D.A. (1997). Inhibition of hyperalgesia by ablation of lamina I spinal neurons expressing the substance P receptor. *Science* 278, 275–279.
- Melzack, R., and Wall, P.D. (1965). Pain mechanisms: a new theory. *Science* 150, 971–979.
- Mihic, S.J., Ye, Q., Wick, M.J., Koltchine, V.V., Krasowski, M.D., Finn, S.E., Mascia, M.P., Valenzuela, C.F., Hanson, K.K., Greenblatt, E.P., et al. (1997). Sites of alcohol and volatile anaesthetic action on GABA(A) and glycine receptors. *Nature* 389, 385–389.
- Mirabile, A., Brioschi, E., Ducceschi, M., Piva, S., Lazzari, C., Bulotta, A., Vigano, M.G., Petrella, G., Gianni, L., and Gregorc, V. (2019). PD-1 inhibitors-related neurological toxicities in patients with non-small-cell lung cancer: a literature review. *Cancers (Basel)* 11, 296.
- Moore, K.A., Kohno, T., Karchewski, L.A., Scholz, J., Baba, H., and Woolf, C.J. (2002). Partial peripheral nerve injury promotes a selective loss of GABAergic inhibition in the superficial dorsal horn of the spinal cord. *J. Neurosci.* 22, 6724–6731.
- Nichols, M.L., Allen, B.J., Rogers, S.D., Ghilardi, J.R., Honore, P., Luger, N.M., Finke, M.P., Li, J., Lappi, D.A., Simone, D.A., et al. (1999). Transmission of chronic nociception by spinal neurons expressing the substance P receptor. *Science* 286, 1558–1561.
- Nishimura, H., Nose, M., Hiai, H., Minato, N., and Honjo, T. (1999). Development of lupus-like autoimmune diseases by disruption of the PD-1 gene encoding an ITIM motif-carrying immunoreceptor. *Immunity* 11, 141–151.
- Paul, J., Zeilhofer, H.U., and Fritschy, J.M. (2012). Selective distribution of GABA(A) receptor subtypes in mouse spinal dorsal horn neurons and primary afferents. *J. Comp. Neurol.* 520, 3895–3911.
- Pirker, S., Schwarzer, C., Wieselthaler, A., Sieghart, W., and Sperk, G. (2000). GABA(A) receptors: immunocytochemical distribution of 13 subunits in the adult rat brain. *Neuroscience* 101, 815–850.
- Shinohara, T., Taniwaki, M., Ishida, Y., Kawaichi, M., and Honjo, T. (1994). Structure and chromosomal localization of the human PD-1 gene (PDCD1). *Genomics* 23, 704–706.
- Sieghart, W., Fuchs, K., Tretter, V., Ebert, V., Jechlinger, M., Hoyer, H., and Adamiker, D. (1999). Structure and subunit composition of GABA(A) receptors. *Neurochem. Int.* 34, 379–385.
- Talbot, S., Foster, S.L., and Woolf, C.J. (2016). Neuroimmunity: physiology and pathology. *Annu. Rev. Immunol.* 34, 421–447.
- Todd, A.J. (2010). Neuronal circuitry for pain processing in the dorsal horn. *Nat. Rev. Neurosci.* 11, 823–836.
- van Bussel, M.T.J., Beijnen, J.H., and Brandsma, D. (2019). Intracranial antitumor responses of nivolumab and ipilimumab: a pharmacodynamic and pharmacokinetic perspective, a scoping systematic review. *BMC Cancer* 19, 519.
- Wang, K., Gu, Y., Liao, Y., Bang, S., Donnelly, C.R., Chen, O., Tao, X., Miranda, A.J., Hilton, M.J., and Ji, R.R. (2020a). PD-1 blockade inhibits osteoclast formation and murine bone cancer pain. *J. Clin. Invest.* 130, 3603–3620.
- Wang, Z., Jiang, C., He, Q., Matsuda, M., Han, Q., Wang, K., Bang, S., Ding, H., Ko, M.C., and Ji, R.R. (2020b). Anti-PD-1 treatment impairs opioid antinociception in rodents and nonhuman primates. *Sci. Transl. Med.* 12, eaaw6471.
- Zeilhofer, H.U., Benke, D., and Yevnes, G.E. (2012). Chronic pain states: pharmacological strategies to restore diminished inhibitory spinal pain control. *Annu. Rev. Pharmacol. Toxicol.* 52, 111–133.
- Zeisel, A., Hochgerner, H., Lonnerberg, P., Johnsson, A., Memic, F., van der Zwan, J., Haring, M., Braun, E., Borm, L.E., La Manno, G., et al. (2018). Molecular architecture of the mouse nervous system. *Cell* 174, 999–1014.e22.

iScience, Volume 23

Supplemental Information

PD-1 Regulates GABAergic

Neurotransmission and GABA-Mediated

Analgesia and Anesthesia

Changyu Jiang, Zilong Wang, Christopher R. Donnelly, Kaiyuan Wang, Amanda S. Andriessen, Xueshu Tao, Megumi Matsuda, Junli Zhao, and Ru-Rong Ji

Supplemental Information

Key Resource Table

Transparent Methods

Supplemental References

Figure S1

Figure S2

Figure S3

Figure S4

Key Resource Table

REAGENT or RESOURCE	SOURCE	IDENTIFIER
Animals		
<i>Pdl</i> knockout mice	Jackson laboratory	21157
Sst-IRES-Cre line	Jackson laboratory	13044
Vglut2- IRES-Cre line	Jackson laboratory	16963
Vgat- IRES-Cre line	Jackson laboratory	16962
Ai32 line	Jackson laboratory	12569
Ai14 line	Jackson laboratory	007909
Antibodies		
Anti PD1 rabbit 1:300	Sigma	PRS4065
anti-NeuN mouse 1:250	Millipore	MAB377
anti-pERK 1:1000	Cell signaling tech	9101
anti-IgG4-FITC 1:200	Abcam	99281
Anti GABAAR α 1 subunit rabbit 1:1000	Proteintech	12410-1-AP
Anti GABAAR α 2 subunit rabbit 1:1000	Abcam	ab72445
Recombinant Proteins and reagents		
Nivolumab (OPDIVO®)	Bristol-Myers Squibb	
Human IgG4	Abcam	ab183266
SSG	Sigma	567565
U0126	InvivoGen	tlrl-u0126

Contact for reagent and resource sharing

Further information and requests for resources and reagents should be directed to and will be fulfilled by the lead contact, Ru-Rong Ji (ru-rong.ji@duke.edu).

Transparent Methods

Animals. Adult mice (2-3 months of both sexes) were used for the behavioral tests and young mice (5-8 weeks of both sexes) were used for electrophysiological studies. We purchased *Pdl*^{-/-} mice (#021157), *Sst*-IRES-Cre mice (#013044), *Vglut2*-ires-cre mice (#016963), *Vgat*-ires-cre mice (#016962), and Ai32 (#012569) and Ai14 mice (#007909), all with C57BL/6 background, from the Jackson laboratory and maintained these mouse lines at a Duke University animal facility in a 12h light/dark cycle with access to food and water ad libitum. Cre lines were crossed with Ai32 mice for optogenetic experiments and with Ai14 mice for immunostaining experiments or targeted electrophysiological experiments. All the mouse procedures were approved by the Institutional Animal Care & Use Committee of Duke University. Animal experiments were conducted in accordance with the National Institutes of Health Guide for the Care and Use of Laboratory Animals.

Spinal Cord or Brain Slices Preparation. Mice of both sexes (5-7 weeks old) were anesthetized with urethane (1.5-2.0 g/kg, i.p.). The lumbosacral spinal cord or the brain was quickly taken out and placed in ice-cold dissection solution (Sucrose 240 mM, NaHCO₃ 25 mM, KCl 2.5 mM, NaH₂PO₄ 1.25 mM, CaCl₂ 0.5 mM and MgCl₂ 3.5 mM), equilibrated with 95% O₂ and 5% CO₂. Transverse spinal slices (400 μm) or brain slices (300 μm) were cut with a vibrating microslicer (VT1200s Leica). The slices were incubated at 34°C for 30 min in ACSF (NaCl 126 mM, KCl 3 mM, MgCl₂ 1.3 mM, CaCl₂ 2.5 mM, NaHCO₃ 26 mM, NaH₂PO₄ 1.25 mM and glucose 11 mM), equilibrated with 95% O₂ and 5% CO₂, before recording (Wang et al., 2020). For inducing PD-1 blockade the slices were incubated with Nivolumab or IgG before using.

Whole-Cell Patch-Clamp Recording. Spinal cord or brain slices were placed in a recording chamber and perfused at a flow rate of 2-4 ml/min with ACSF which was saturated with 95% O₂ and 5% CO₂ and maintained at room temperature. Whole-cell voltage-clamp recordings were performed with patch-pipettes fabricated from thin-walled, fiber-filled capillaries. Patch-pipette solution used in this study contained: Cs₂SO₄ 110, CaCl₂ 0.5, MgCl₂ 2, EGTA 5, HEPES 5, Mg-ATP 5, tetraethylammonium (TEA)-Cl 5 (pH 7.3, adjusted with KOH, 300mOsm). The patch-pipettes had a resistance of 8–10 MΩ. The holding potential (V_H) was set to 0 mV when whole-

cell patch-clamp was made. The GABAergic currents, spontaneous or evoked inhibitory postsynaptic currents (IPSCs) were recorded in the presence of strychnine (1 μ M), AP-5 (50 μ M) and CNQX (10 μ M).

To analyze the unit current, membrane capacitance (C_m) of recorded neuron was determined through injection of hyperpolarizing current steps (2 s, -5 pA increments, delivered every 10 s). Unit currents (pA/pF) were determined by dividing the peak amplitude of current by the cell membrane capacitance.

Signals were acquired using an Axopatch 700B amplifier. The data were stored and analyzed with a personal computer using pCLAMP 10.3 software. Spontaneous IPSC events were detected and analyzed using Mini Analysis Program ver. 6.0.3. Outward currents were measured by Clampfit. Briefly, the current value was calculated by the peak amplitude value of an outward current subtracted the amplitude value of baseline under voltage-clamp configuration.

Drug Applications. Exogenous GABA, THIP or glycine was applied locally for 500 ms by patch micropipette.

Dorsal Root-Evoked IPSCs. The evoked IPSCs were elicited by stimulating the dorsal root. In brief, the stimulation was performed by using a microelectrode (FHC, #30203). The strength of the stimuli (duration: 0.1 ms) used was 1.2 times the threshold to elicit IPSCs (Kato et al., 2004)

Light-Evoked IPSCs. For optogenetic activation of inhibitory interneurons, vGAT^{Ai32} mice were used. Blue light (473 nm wavelength) illumination (0.1 s) was delivered through a 40X water-immersion microscope (BX51WIF; Olympus) objective to induce a light-evoked response. The interval of the paired pulse of the light was set to 80 ms. Following identification of vGAT-positive or negative neurons, we implemented a recovery period of 10-15 min before recording to allow neurons to recover from blue light exposure (Pagani et al., 2019).

Immunohistochemistry. Mice of both sexes (7-8 weeks old) were deeply anesthetized with isoflurane, followed by the perfusion of PBS and in turn 4% paraformaldehyde (PFA)/1.5% picric acid. After the perfusion, lumbar spinal cord (L3-L5) were removed and post-fixed for 2h at room temperature. The tissues were washed several times in PBS, followed by cryopreservation in 20%

sucrose overnight followed by 30% sucrose overnight. The samples were sliced into sections (20 μm) in a cryostat. For the anti-Nivolumab and/or anti-pERK staining after Nivolumab (300 ng/mL or 1000ng/mL) incubation on living spinal cord slices (200 μm), the slices were post-fixed overnight and then dehydrated in 30% sucrose for 12 h.

The sections or slices were blocked with 10% donkey serum with 0.3% Triton X-100 for 1 h at room temperature and then incubated overnight at 4°C with the following primary antibodies: anti-PD1 antibody (rabbit, 1:300, Sigma, Cat: PRS4065), anti-NeuN antibody (mouse, 1:250, Millipore, Cat: MAB377) and/or anti-pERK (rabbit, 1:1000, Cell signaling tech, Catalog: 9101). After washing, the sections were incubated with Cy3-, Cy5-conjugated secondary antibodies (1:500; Jackson ImmunoResearch) and/or anti-IgG4-FITC (1:200, Abcam, catalog: 99281) at 4°C overnight. Nissl (1:200, Invitrogen, cat: N21483) was used for 2 hours for visualizing neurons and DAPI was contained in mounting medium (Sigma, Cat: SLCC8848) to stain cell nuclei. Three sections were analyzed in each mouse and 4 mice per group were analyzed.

For the anti-Nivolumab staining after Nivolumab (300 ng/mL) incubation on living cultured cortical neurons, the neurons on coverslips were post-fixed in 4% PFA for 15 min and incubated in 0.3% Triton X-100 containing PBS for 1 hour, followed by incubation with the following primary antibodies: anti-PD1 antibody (rabbit, 1:300, Sigma, Cat: PRS4065) and anti-NeuN antibody (mouse, 1:250, Millipore, Cat: MAB377). After washing, the neurons were incubated with Cy3-, Cy5-conjugated secondary antibodies (1:500; Jackson ImmunoResearch) and/or anti-IgG4-FITC (1:200, Abcam, catalog: 99281) at 4°C overnight. DAPI was contained in mounting medium (Sigma, Cat: SLCC8848) to stain cell nuclei.

The images were examined with a ZEISS LSM 880 confocal microscope. To confirm the specificity of PD-1 antibody, blocking experiments were conducted in brain sections using a mixture of anti-PD-1 antibody (1:300) and immunizing blocking peptide (1:300, Sigma, Catalog: SBP4065), based on a protocol recommended for blocking with immunizing peptide (www.abcam.com/technical). The specificity of PD-1 antibody was also tested in *Pdl* knockout mice, as we previously reported (Wang et al., 2020).

In Situ Hybridization. Mice were deeply anesthetized with isoflurane and transcardially perfused with PBS followed by 4% PFA/1.5% picric acid. Following perfusion, lumbar spinal cords (L3-L5) were removed and post-fixed for 2h at room temperature. The tissues were washed several

times in PBS, followed by cryopreservation in 20% sucrose overnight followed by 30% sucrose overnight. Spinal cords were then embedded in optimal cutting temperature (OCT) medium (Tissue-Tek) and cryosectioned to produce 14 μm sections which were mounted onto Superfrost Plus charged slides (VWR). Importantly, each slide contained both *Pdcd1*^{+/+} and *Pdcd1*^{-/-} sections to control for possible variability in staining between slides and to control for the specificity of the *Pdcd1* probe. *In situ* hybridization was performed using the RNAscope system (Advanced Cell Diagnostics) according to the manufacturer's recommendations using the protocol for the Multiplex Fluorescent Kit version 2. We used probes directed against murine *Pdcd1* (*Pd1*, NM_008798.2, #416781), *Pdl1* (NM_021893.3, #420508-C3) and *Pdl2* (NM_021396.2, 447781-C3), *Slc17a6* (Vglut2, NM_080853.3, #319171-C2) and *Slc32a1* (Vgat, NM_009508.2, #319191-C3). Images were captured using a CCD Spot camera affixed to a Nikon fluorescent microscope (Nikon Eclipse NiE). For higher resolution analysis, images were also captured using a Zeiss LCM 880 confocal microscope with a z-step size of 1 μm and maximum projections were subsequently produced using the Zeiss ZEN software program. Images were taken across animals and genotypes using the same acquisition settings (Wang et al., 2020).

Primary Cultures of Cortical Neurons. Primary cultures of cortical neurons were prepared from embryonic day 17-19 (E17-19) WT or *Pdl1*^{-/-} mice. Embryos were removed from maternal mice anesthetized with isoflurane and euthanized by decapitation. Cortices were dissected and placed in Ca^{2+} and Mg^{2+} free Hank's balanced salt solution (HBSS, GIBCO) and digested at 37 °C in humidified O_2 incubator for 30 min with collagenase type II (Worthington, 285 units/mg, 12 mg/ml final concentration) and dispase II (Roche, 1 unit/mg, 20 mg/ml) in HBSS (pH 7.3). Digestion was terminated by fetal bovine serum-containing DMEM (GIBCO). Cortex were mechanically dissociated using fire-polished pipettes, filtered through a 100- μm nylon mesh and centrifuged (1,000 g for 5 min). The pellet was resuspended and plated on poly-D-Lysine/Laminin coated glass coverslips (CORNING), and cells were plated in DMEM containing 5% fetal bovine serum, 1% penicillin and streptomycin. After 5-6 h, primary cultures were switched to Neurobasal Plus medium containing 2% B27 supplement, 1% GlutaMAX-I, 1% penicillin and streptomycin (GIBCO). Three days after plating, cytosine arabinoside was added to a final concentration of 10 μM to curb glial proliferation. Whole-cell recoding and immunostaining experiments were conducted on DIV 7-8.

Western Blot. The spinal or brain tissues were homogenized in a lysis buffer containing protease and phosphatase inhibitors at 4°C for 30 min. After centrifugation, the protein concentrations were measured using the BCA protein assay kit (Pierce, Thermo Fisher Scientific). Then protein (50 µg) was loaded for each lane and separated by SDS-PAGE gel (4-20%; Bio-Rad). After the transfer, the blots were incubated overnight at 4°C with polyclonal antibodies against GABA_AR α1 subunit (rabbit, 1:1000, Proteintech, Catalog: 12410-1-AP) and polyclonal antibodies against GABA_AR α2 subunit (rabbit, 1:1000, abcam, Catalog: ab72445). For the loading control, the blots were probed with GAPDH antibody (1:5000, mouse, Proteintech, catalog: 60004-1-1g). The blots were then incubated with an HRP-conjugated secondary antibody and developed in ECL solution (Pierce, Thermo Fisher Scientific). Chemiluminescence signal was revealed by Bio-Rad ChemiDoc XRS for 1 to 3 minutes. Specific bands were evaluated according to apparent molecular sizes.

Mouse Model of Inflammatory Pain. Inflammatory pain was induced by complete Freund's adjuvant (CFA, Sigma) via intraplantar injection (20 µL) into a hind paw under brief anesthesia with isoflurane.

Mouse Model of Neuropathic Pain. Neuropathic pain was induced by partial sciatic nerve ligation (pSNL). To produce pSNL, the sciatic nerve was exposed under isoflurane, and a tight ligation of approximately one-third to one-half of the diameter of the left sciatic nerve was performed with 6-0 silk suture.

Von Frey Testing for Mechanical Allodynia. Mice were habituated to the environment for at least 2 days before the testing. All the behaviors were tested blindly. For testing mechanical allodynia, we confined mice in boxes (14 × 18 × 12 cm) placed on an elevated metal mesh floor and stimulated their hind paws with a series of von Frey hairs with logarithmically increasing stiffness (0.16-2.00 g, Stoelting), presented perpendicularly to the central plantar surface. We determined the 50% paw withdrawal threshold by Dixon's up-down method (Dixon, 1980).

Intracerebroventricular injection

For stereotaxic surgery, mouse was anesthetized with isoflurane and the head was fixed in a stereotaxic apparatus (Narishige scientific instrument lab.). A guide cannula (62004, RWD Life Science) was stereotaxically implanted into the left lateral ventricles (AP: -0.3 mm; ML: +1.3 mm; V: -2.0 mm) according to the mouse brain atlas¹⁶. After four-day recovery, an infusion needle (62204, RWD Life Science) was inserted into lateral ventricles through the guide cannula to a depth of 2.5 mm for IgG or Nivolumab injection. Following the completion of the infusion, the needle was left for an additional 2 min to limit reflux.

Fraction of Loss of Righting Reflex (LORR). Mice were placed in a cylindrical gas-tight, controlled-environment chamber. After 90 min of habituation with 100% oxygen flowing (at a rate of 5 L/min) each day on two successive days, anesthesia was induced. Anesthetic gas concentrations were determined in triplicate by a gas indicator (Riken FI-8000). The isoflurane concentration was set from 0.55% to 1.2% (an increment of 0.05%) for 15 min, and each animal's righting reflex was assessed by gently rolling the chamber until the mouse was placed on its back during the last 2 min. At each concentration, a mouse was considered to have lost the righting reflex if it did not turn itself prone onto all four limbs within 2 min. To minimize the number of anesthetic exposures, each mouse was only exposed to isoflurane two times and the intervals were more than 2 days. Mouse temperature was maintained between $36.6 \pm 0.6^{\circ}\text{C}$ (McCarren et al., 2013).

Assess the Duration of Induction and Emergence of Anesthesia. For the isoflurane anesthesia, isoflurane was set to a certain concentration in the chamber. The duration of induction (seconds) was determined when the mouse lost its righting reflex from the time it was put into the chamber. The duration of emergence (seconds) was defined from time the isoflurane was turn off until the time mouse regained its righting reflex. For the pentobarbital anesthesia, pentobarbital was injected intraperitoneally (40 mg/kg) (Kelz et al., 2008; McCarren et al., 2013).

Statistical Analyses. All the data were expressed as mean \pm SEM. Statistical analyses were completed with Prism GraphPad 8.0. Biochemical, electrophysiology and behavioral data were analyzed using two-tailed unpaired *t*-test (two groups) or Two-Way ANOVA followed by

Bonferroni post-hoc test. The criterion for statistical significance was $P < 0.05$. In all cases of electrophysiology recordings, n refers to the number of the neurons studied.

Supplemental References

Dixon, W.J. (1980). Efficient analysis of experimental observations. *Annu Rev Pharmacol Toxicol* 20, 441-462.

Kato, G., Furue, H., Katafuchi, T., Yasaka, T., Iwamoto, Y., and Yoshimura, M. (2004). Electrophysiological mapping of the nociceptive inputs to the substantia gelatinosa in rat horizontal spinal cord slices. *J Physiol* 560, 303-315.

Kelz, M.B., Sun, Y., Chen, J., Cheng Meng, Q., Moore, J.T., Veasey, S.C., Dixon, S., Thornton, M., Funato, H., and Yanagisawa, M. (2008). An essential role for orexins in emergence from general anesthesia. *Proc Natl Acad Sci U S A* 105, 1309-1314.

McCarren, H.S., Moore, J.T., and Kelz, M.B. (2013). Assessing changes in volatile general anesthetic sensitivity of mice after local or systemic pharmacological intervention. *J Vis Exp*, e51079.

Pagani, M., Albisetti, G.W., Sivakumar, N., Wildner, H., Santello, M., Johannssen, H.C., and Zeilhofer, H.U. (2019). How Gastrin-Releasing Peptide Opens the Spinal Gate for Itch. *Neuron* 103, 102-117 e105.

Wang, Z., Jiang, C., He, Q., Matsuda, M., Han, Q., Wang, K., Bang, S., Ding, H., Ko, M.C., and Ji, R.R. (2020). Anti-PD-1 treatment impairs opioid antinociception in rodents and nonhuman primates. *Sci Transl Med* 12.

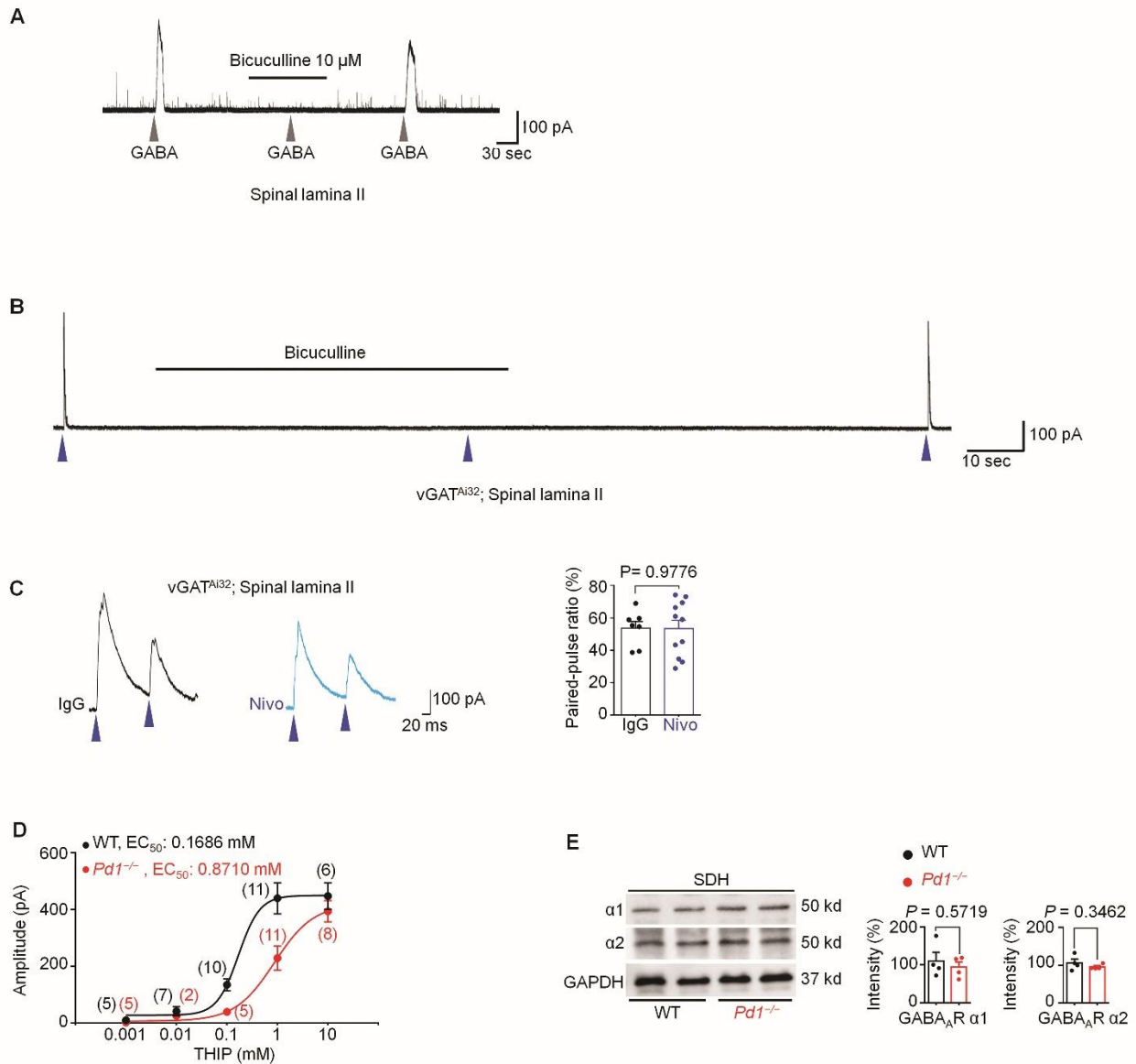


Figure S1. Loss of PD-1 function impairs GABA_AR-mediated currents in spinal cord slice.

Related to Figure 1.

(A) Blockade of GABA (1 mM) current in spinal lamina II neurons by the GABA_AR antagonist bicuculline.

(B) Blockade of blue light-induced currents by bicuculline in lamina II neurons from vGAT^{Ai32} mice.

(C) Left: example traces of paired pulse blue light-evoked currents in spinal lamina II neurons of vGAT^{Ai32} mice showing the effect of IgG or Nivo (300 ng/mL, 2 h). Right: quantification of the

amplitude of the 2nd currents relative to the 1st currents. n = 7 and 11 neurons from 3 animals per group.

(D) Dose-response curve showing average amplitudes of THIP-induced currents in SDH lamina II neurons of WT and *Pdl*^{-/-} mice. The curves were drawn according to the Hill equation. Values in parentheses denote the number of recorded neurons from 3-4 animals per group.

(E) Left: Representative immunoblots showing the expression of $\alpha 1$ and $\alpha 2$ subunits of GABA_AR in the lumbar spinal cord from WT and *Pdl*^{-/-} mice. Right: quantification of GABA_AR $\alpha 1$ and $\alpha 2$ immunoblots (normalized to GAPDH) in WT and *Pdl*^{-/-} mice. n = 4 animals/group.

Gray arrowheads indicate the application of GABA. Blue arrowheads indicate the blue light stimulus. $V_H = 0$ mV. Unpaired two-tailed t-test. All error bars indicate the mean \pm SEM.

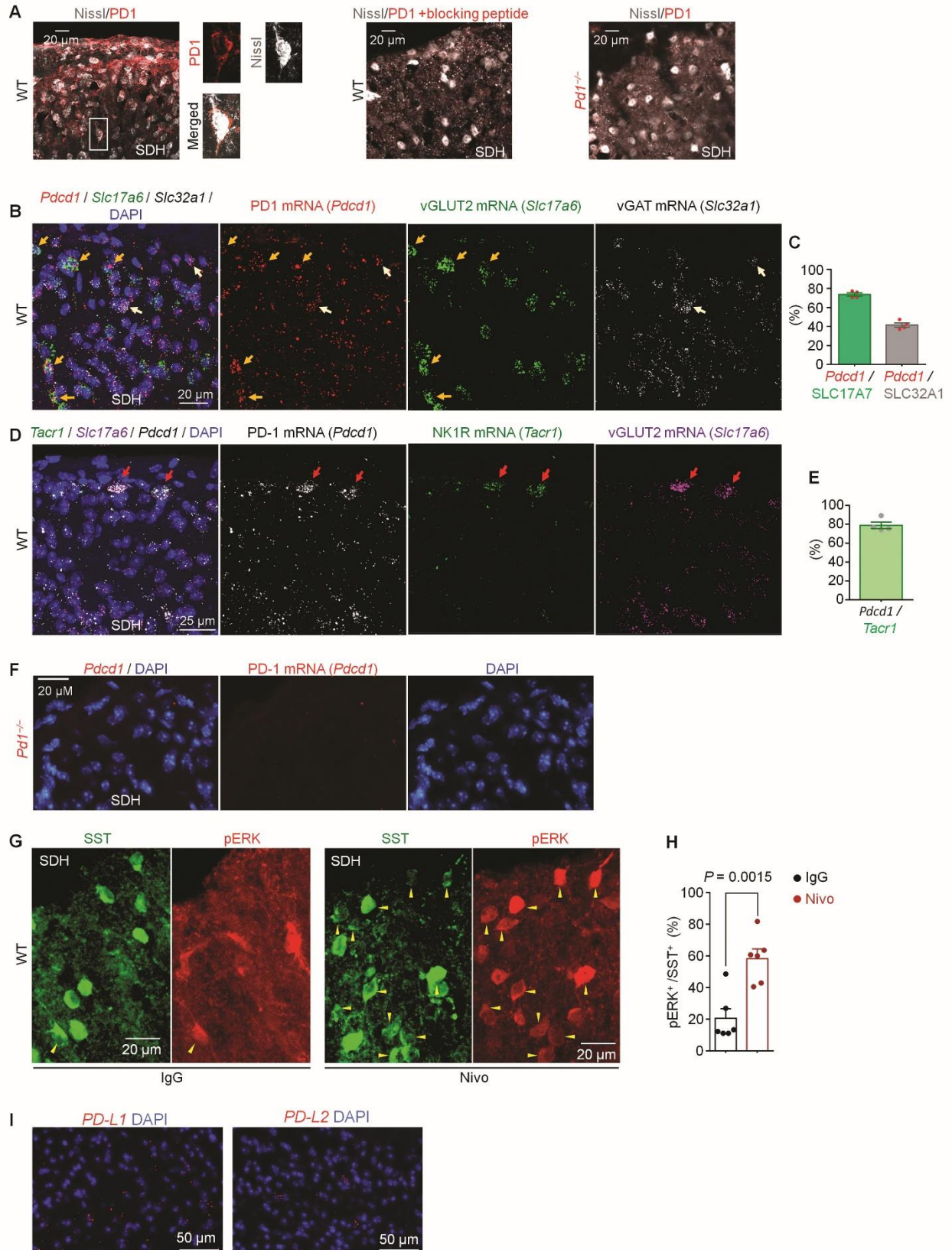


Figure S2. Characterization of *Pdl* mRNA and PD-1 protein expression in SDH neurons. Related to Figure 2.

(A) Transverse sections of SDH showing double staining of PD-1 (red) and Nissl (gray) in WT mice with the box enlarged (left), in WT mice in the presence of a blocking peptide (middle) and in *Pdl*^{-/-} mice (right). Note that PD-1 immunostaining is lost after treatment of the blocking peptide and in KO mice.

(B,C) ISH shows mRNA expression of *Pdcd1* (= *pdl*, red) in excitatory neurons (*Slc17a6* for vGLUT2, green) and inhibitory neurons (*Slc32a1* for vGAT, white) of SDH. (B) Typical images. DAPI staining labels nuclei in SDH. (C) Percentage expression of *Pdl* in SDH excitatory and inhibitory neurons. n = 4 mice/group. Note there is more PD-1 expression in excitatory neurons (orange arrows) than in inhibitory neurons (yellow arrows) in SDH.

(D,E) ISH shows *Pdcd1* mRNA expression in SDH projection neurons (*Tacr1* for NK-1, green) and excitatory neurons (*Slc17a6* for vGLUT2, purple). (D) Typical images. Red arrows indicate projection neurons with triple staining. (E) Percentage expression of *Pdl* in SDH projection neurons. n = 4 mice/group.

(F) ISH shows absence of *Pdcd1* mRNA expression in SDH of *Pdl*^{-/-} mice.

(G,H) Nivolumab-induced pERK expression in SDH neurons of SST reporter mice. (H) Double staining of pERK (red) and SST (green). (I) Quantification of pERK in SST⁺ neurons. n = 6 slices from 3-4 mice per group. Spinal cord slices were prepared from SST^{tdTomato} mice, incubated with IgG or Nivo (300 ng/mL) for 2 h, and then fixed for immunostaining.

(I) ISH shows PD-L1 and PD-L2 mRNA expression in SDH.

All error bars indicate the mean ± SEM.

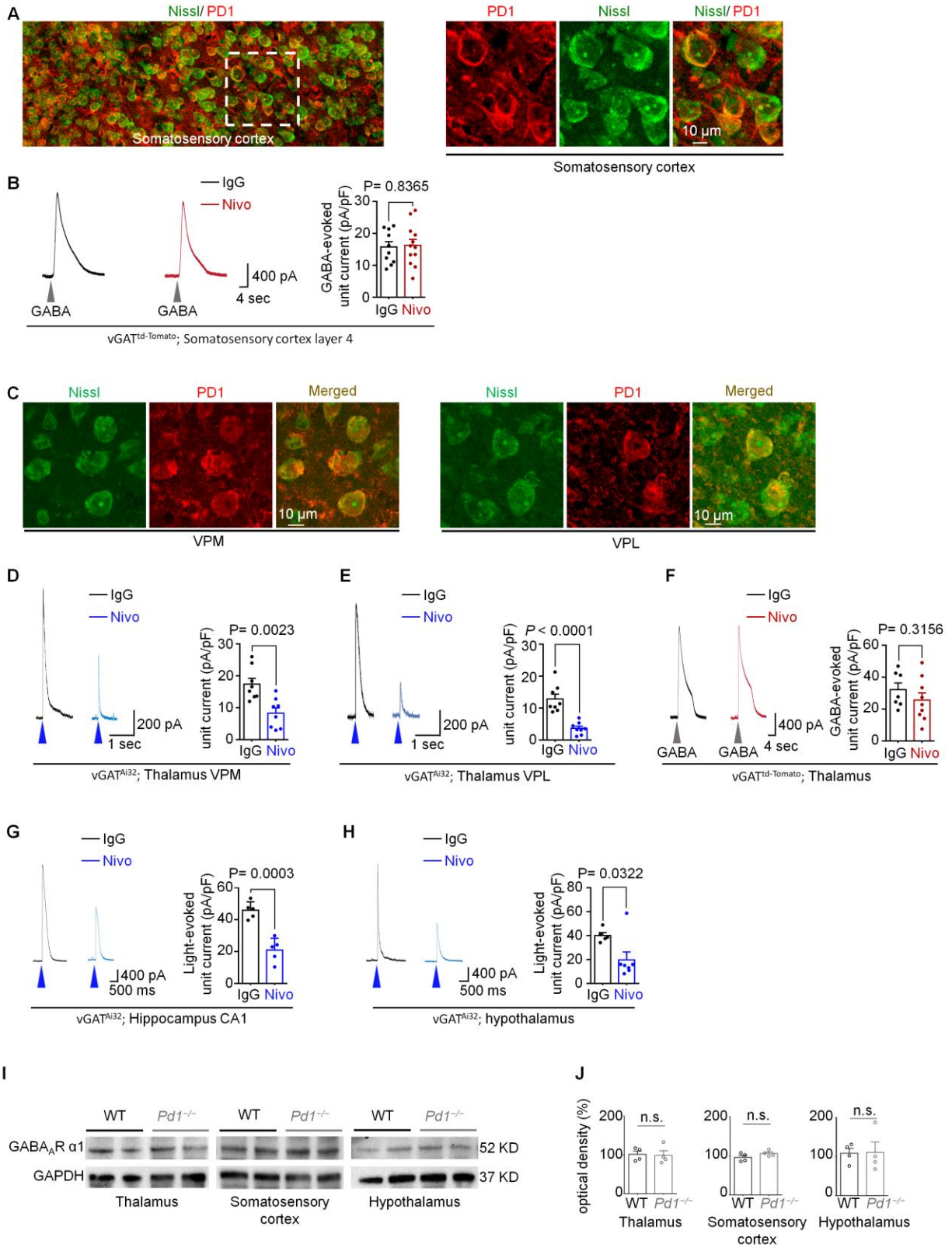


Figure S3. Characterization of PD-1 expression, GABA_AR-mediated currents, and GABA_AR expression in different brain regions. Related to Figure 3.

(A) Double staining of PD-1 (red) and Nissl (green) in S1 somatosensory cortex. Right: higher magnification images of the dashed box. Note PD-1 is present on the surface of cortical neurons.

(B) GABA (1 mM) induced currents from vGAT⁺ neurons in S1-layer IV of Vgat reporter mice following incubation with IgG or Nivo (300 ng/mL, 2 h). Right: unit currents of GABA. n = 10 and 12 neurons from 3 animals/group.

(C) Double staining of PD-1 (red) and Nissl (green) in S1, thalamus VPM (left) and VPL (right).

(D-H) Effects of Nivolumab and IgG (300 ng/ml, 2 h) on light-evoked and GABA-evoked (F) currents and in vGAT-negative neurons of vGAT^{Ai32} mice or vGAT^{tdTomato} mice (F).

(D,E) Light-evoked GABA currents in VPM neurons (D) and VPL neurons (E). Left: Traces of light-induced currents. Right: unit currents. n = 7 and 9 neurons from 3 animals/group (D). n = 9 and 7 neurons from 3 animals/group (E).

(F) GABA (1 mM) induced currents in thalamic neurons from vGAT^{tdTomato} mice. Left, traces of currents. Right: unit currents. n = 7 and 9 from 3 animals/group.

(G,H) Light-evoked GABA currents from hippocampal CA1 neuronal (G) and hypothalamic neurons (H). n = 5 neurons from 3 animals/group (G). n = 5 and 7 neurons from 3 animals/group (H).

(I,J) Western blot shows GABA_AR expression in different brain regions of WT and *Pdl1*^{-/-} mice.

(I) Western gels showing the expression of $\alpha 1$ subunits of GABA_AR in the thalamus, somatosensory cortex and hypothalamus. (J) Quantification of band density of $\alpha 1$ -GABA_AR (normalized to GAPDH). n = 4 mice/group.

Unpaired two-tailed t-test. All error bars indicate the mean \pm SEM.

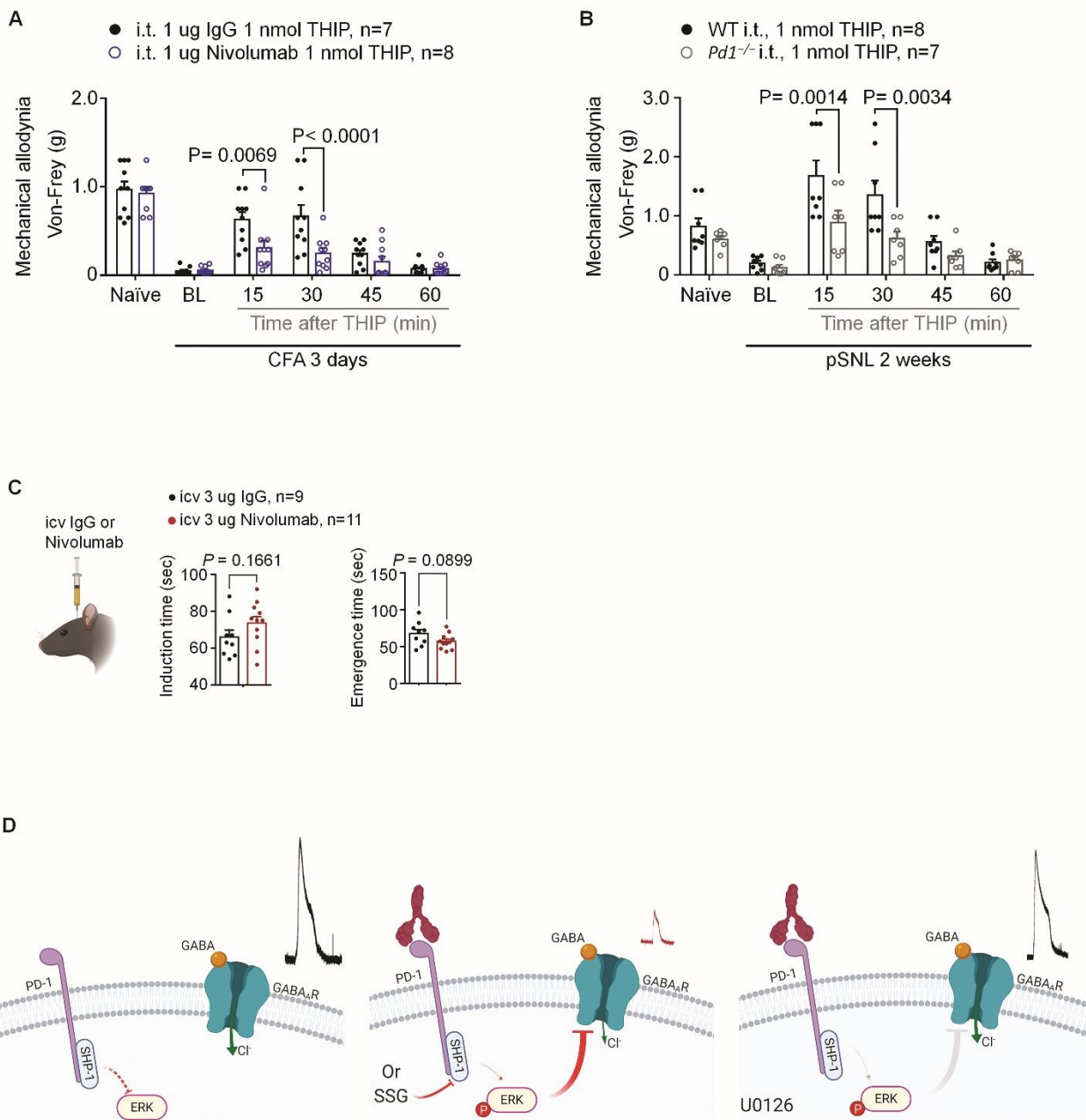


Figure S4. Further characterization of GABA-mediated analgesia after PD-1 blockade and the schematic of PD-1 regulation of GABAergic transmission. Related to Figure 4.

(A) Von Frey testing showing the effect of IgG or Nivo pre-treatment (1 μ g, i.t.) on intrathecal THIP (1 nmol) induced inhibition of inflammatory pain in CFA-inflamed mice. $P < 0.0001$, $P = 0.0069$, IgG4 + THIP versus nivolumab + THIP, two-way ANOVA, followed by Bonferroni's post hoc test.

(B) Von Frey testing showing the effect of intrathecal THIP (1 nmol) on neuropathic pain in the sciatic nerve ligation (pSNL) model in WT and *Pdl*^{-/-} mice. $P = 0.0014$, $P = 0.0034$, WT versus *Pdl*^{-/-}, two-way ANOVA, followed by Bonferroni's post hoc test.

(C) Left: a schematic diagram of intracerebroventricular injection. Middle and Right: the effects of 1.5% isoflurane on the induction time (middle) and emergence time (right) in IgG- and Nivolumab-treated mice (n = 9-11 animals in each group).

(D) Schematic illustration of the proposed mechanism by which PD-1 potentiates GABAergic neurotransmission in SDH. Left, under the normal conditions, PD-1 suppresses ERK activation via SHP-1, thereby enabling GABA_AR-mediated synaptic transmission. Middle, inhibition of PD-1 signaling using anti-PD1 neutralizing antibodies (e.g. Nivolumab) or SHP-1 inhibitors (SSG) leads to activation of ERK (pERK), which in turn suppresses GABA_AR-mediated currents. Right, inhibition of the pERK pathway with U0126, in turn, relieves pERK suppression of GABA_AR function, and thus, restores the normal GABAergic neurotransmission.

All error bars indicate the mean \pm SEM.